All Members of the Arabidopsis DGAT and PDAT Acyltransferase Families Operate During High and Low Temperatures

Zachery D. Shomo[1], Samira Mahboub[1], Hathaichanok Vanviratikul[2], Mason McCormick[1], Tatpong Tulyananda[3], Rebecca L. Roston[1,†,*], and Jaruswan Warakanont[2,†,*]

[1]Center for Plant Science Innovation, Department of Biochemistry, University of Nebraska-Lincoln, NE 68588; [2]Department of Botany, Kasetsart University, Chatuchak, Bangkok 10900 Thailand; [3]School of Bioinnovation and Bio-Based Product Intelligence, Faculty of Science, Mahidol University, Bangkok 10400 Thailand

*Authors for correspondence

*Rebecca L. Roston

Center for Plant Science Innovation, Department of Biochemistry

1901 Vine Street, N123

Lincoln NE, 68588

Tel: 1-402-472-2936

Email: rroston@unl.edu

and

*Jaruswan Warakanont

Department of Botany, Faculty of Science, Kasetsart University

50 Ngamwongwan Rd., Chatuchak, Bangkok Thailand 10900

Tel: 668-6412-9360

Email: jaruswan.w@ku.th

†These authors contributed equally to this work

Running head: TAG and temperature tolerance in Arabidopsis

One sentence summary: The link between TAG accumulation and temperature tolerance was studied by stressing Arabidopsis acyltransferase muatants, revealing that the two are not tightly linked.

Abstract

The accumulation of triacylglycerol (TAG) in vegetative tissues is necessary to adapt to changing temperatures. It has been hypothesized that TAG accumulation is required as a storage location for maladaptive membrane lipids. The TAG acyltransferase family has five members (DGAT1/2/3 and PDAT 1/2), and their individual roles during temperature challenges were either described conflictingly or not at all. Therefore, we used *Arabidopsis thaliana* loss of function mutants in each acyltransferase to investigate the effects of temperature challenge on TAG accumulation, plasma membrane integrity, and temperature tolerance. All mutants were tested under one high- and two low-temperature regimens, during which we quantified lipids, assessed temperature sensitivity, and measured plasma membrane electrolyte leakage. Our findings revealed reduced effectiveness in TAG production during at least one temperature regimen for all acyltransferase mutants compared to the wildtype, resolved conflicting roles of *pdat1* and *dgat1* by demonstrating their distinct temperature-specific actions, and uncovered that plasma membrane integrity and TAG accumulation do not always coincide, suggesting a multifaceted role of TAG beyond its conventional lipid reservoir function during temperature stress.

Introduction

The ability of a plant to adapt and overcome environmental stressors is one of the strongest tools in its arsenal. However, as the climate continues to change, plants have become increasingly challenged by unseasonable temperature events, leading to decreases in agricultural yields and financial losses (Burke and Emerick, 2016; Cohen et al., 2021). To prepare for temperature changes, plants acclimate via exposure to non-lethal temperatures triggering molecular remodeling to survive more severe conditions in both freezing (Wanner and Junttila, 1999), and heat (Lindquist, 1986). If acclimation is interrupted, plants become susceptible to temperatures at which they would otherwise survive (Gusta et al., 2009).

During high and low temperatures, triacylglycerol (TAG) accumulates in leaves and is essential for survival (Mueller et al., 2017; Arisz et al., 2018; Tan et al., 2018); however, the reason for TAG accumulation is unclear. Several hypotheses have been proposed to explain this phenomenon. First, TAG could accumulate as an energy reserve to aid in recovery from temperature stress by producing ATP via β-oxidation. Studies in *Chlamydomonas reinhardtii* showed that TAG accumulates rapidly in response to nitrogen deprivation but quickly degrades after adding back nitrogen, coinciding with the resynthesis of organellar membranes (*reviewed by* Li-Beisson et al., 2015). Second, TAG may accumulate to prevent oxidative damage to the photosystems during high heat and freezing conditions. Oxidation of thylakoid membrane lipids occurs in *Chlamydomonas reinhardtii* (Du et al., 2018) and Arabidopsis (Schmid-Siegert et al., 2016), and if not removed cause reductions in photosynthetic efficiency (Yu et al., 2021). Third, TAG could serve as a reservoir for damaged and remodeled membrane lipids that could compromise membrane integrity if not removed (*reviewed by* Lu et al., 2020). Support for this hypothesis comes from the increase in plastid-derived fatty acids that appear in TAG during temperature stresses due to specific remodeling enzymes. During heat stress, HEAT-INDUCIBLE LIPASE1 removes fluidizing polyunsaturated fatty acids from the plastid that are stored as TAG (Higashi et al., 2018). Similarly during freezing, SENSITIVE TO FREEZING2 (SFR2) remodels the outer envelope of the chloroplast ultimately moving monogalactosyldiacylglycerol (MGDG) backbones into TAG (Moellering et al., 2010).

In each of these scenarios, TAG accumulation is related to maintaining interorganellar and plasma membrane integrity. A stable membrane provides one of the first lines of defense against damage to cell permeability and organellar leakage. To maintain fluidity, the types of lipids incorporated into membranes must change. During low temperatures, the levels of rigidifying lipids decrease (Miquel et al., 1993; Ghosh et al., 2021), whereas in high temperatures the incorporation of rigidifying lipids is favored (Falcone et al., 2004; Shiva et al., 2020; Guihur et al., 2022). In both cases, unfavorable, damaged, or oxidized lipids are removed via membrane remodeling to modify the degree of fatty acid

saturation and headgroup abundance. These byproducts can be toxic and lead to programmed cell death during heat (Fan et al., 2013a; Higashi et al., 2018) and chloroplast damage during freezing (Moellering et al., 2010). Approximately four percent of fatty acids are degraded via turnover pathways per day (Bao et al., 2000). Because temperature stress can occur within hours, plants need alternatives to *de novo* synthesis pathways to quickly store remodeled fatty acids.

In Arabidopsis, there are two families of acyltransferases that generate TAG: the DIACYLGLYCEROL ACYLTRANSFERASES (DGAT1, 2, and 3) and PHOSPHOLIPID: DIACYLGLYCEROL ACYLTRANSFERASES (PDAT1 and PDAT2). The DGAT family catalyzes the transfer of soluble acyl-CoA with diacylglycerol (DAG) to produce TAG (Liu et al., 2012). DGAT1 and DGAT2 have been shown to be membrane-bound in the endoplasmic reticulum (ER) (**Fig. 1A**, Shockey et al., 2006), whereas the subcellular location of soluble DGAT3 has been contended (Saha et al., 2006; Aymé et al., 2018; Carro et al., 2022). PDATs are membrane-bound in the ER and catalyze the transfer of an acyl chain from a phospholipid, primarily phosphatidylcholine (PC) in the ER to DAG, producing TAG and a lyso-phospholipid as a byproduct (**Fig. 1A**, Ståhl et al., 2004; Mhaske et al., 2005).

A loss-of-function mutant in each acyltransferase family was previously shown to affect TAG accumulation and temperature tolerance in either freezing or heat. During heat challenge, *pdat1* mutants accumulated less TAG and had impaired recovery (Mueller et al., 2017). When challenged with freezing conditions, plants lacking *dgat1* were unable to recover and had lower TAG levels, whereas DGAT1 overexpression performed better than wild type (Arisz et al., 2018; Tan et al., 2018). However, a recent study showed PDAT1 overexpression in Arabidopsis also improved low temperature tolerance compared to wild type, and *pdat1* loss-of-function mutants were susceptible (Demski et al., 2020). In these studies, the methods used for plant growth and temperature treatment varied making comparisons of the functions of acyltransferase enzymes in heat and freezing more challenging. The type, temperature, duration, and relative severity of temperature treatments applied to a plant change their physiological responses and tolerance to temperature stress (Lindquist, 1986; Gilmour et al., 1988; Wanner and Junttila, 1999). Together, this suggested that the type of temperature treatment may allow us to tease out the function of all DGAT and PDAT acyltransferase family members during temperature stress.

Therefore, we hypothesized that both DGAT and PDAT family members are required for temperature tolerance and that any changes to TAG accumulation would directly correlate with impaired membrane integrity. To test this, we assayed loss-of-function mutants of Arabidopsis DGAT1, 2, 3, PDAT1, and 2 under the same conditions over a time course (**Fig. 1**). We used the *sfr2-3* mutant as a

control for post-freezing recovery (Barnes et al., 2016). We also used a mutant deficient in MEMBRANE-BOUND O-ACYL TRANSFERASE 5 (MBOAT5) as a control for TAG accumulation. The MBOAT5 enzyme has been shown to catalyze wax biosynthesis (Klypina and Hanson, 2008), and has been renamed LONG-CHAIN-ALCOHOL O-FATTY-ACYLTRANSFERASE 2 (AT2) since we began this work (Wang et al., 2018).

Our goal was to investigate whether the duration and severity of low and high temperatures affect the importance of which acyltransferases respond. We used the resulting dataset to probe coincidence of TAG production and plasma membrane integrity in low temperatures. We found that loss of either DGAT or PDAT enzyme family members can reduce TAG accumulation during temperature stress , confirmed that deficits in TAG accumulation can lead to leaf damage, but that TAG accumulation does not always coincide with plasma membrane integrity.

Results

Previous work reported that a role for multiple acyltransferase mutants could be observed during treatment with high and low temperatures (Mueller et al., 2017; Arisz et al., 2018; Tan et al., 2018; Demski et al., 2020). To encompass all family members, address the apparent conflict between PDAT1 and DGAT1 roles at low temperatures, and explore the relationship of TAG accumulation to temperature tolerance, we subjected Arabidopsis mutants (*dgat1*, *2*, *3*, or *pdat1*, *2*) to two low-temperature and one high-temperature regimen.

The first low-temperature step used multiple, long-term low-temperature steps, where each low temperature was applied at the end of the light cycle, **Fig. 1B**. This and similar assays, commonly used to simulate field conditions experienced by plants, mimic overnight freezing at the end of the relative day (Wanner and Junttila, 1999; Gusta et al., 2009; Moellering et al., 2010; Barnes et al., 2016). It is a non-lethal assay, that allows for scoring of leaf damage and plant recovery. The second low-temperature ramp used a descending temperature ramp, **Fig. 1C**, to rapidly challenge plasma membrane integrity, resembling an unseasonable cold spell (Warren et al., 1996; Thalhammer et al., 2020; Barnes et al., 2023). In both assays, plants were exposed to a low but non-freezing temperature (4°C) for cold acclimation in preparation for subzero freezing temperatures. The high-temperature step, **Fig. 1D**, was based on a previous study that showed a 15-fold increase in some TAG species (Mueller et al., 2017). It used a mild heat stress (37°C) and multiple timepoint samples to capture discrete changes in the TAG profile.

TAG accumulation and recovery of *pdat1* and *dgat1* are uniquely impacted during the cold and freezing

After three weeks of growth during normal conditions, lipids were extracted and relative mole percents (%) of TAG were quantified. The TAG levels were similar in the mutants compared to wild type (**Fig. 2A, i**). After two days at 4°C, *dgat1* mutants only accumulated 1.2% TAG compared to 2.9% in wild type, a difference of 42% (**Fig. 2A, ii**). After one week at 4°C, the percent of TAG in *dgat1* mutants was similar to that of wild type, while the percent of TAG in *pdat1* mutants was slightly increased (**Fig. 2A, iii**). At two hours of -6°C treatment, the TAG levels in all the mutants were equivalent to wild type (**Fig. 2A, iv**). After sixteen hours of -6°C treatment, *pdat1* mutants had 52% less TAG than wild type, while all other mutants accumulated TAG levels similar to wild type. We also checked for any visible phenotypes in any of the acyltransferase mutants following three weeks growth and during the low-temperature regimen

and found none (**Fig. 2B, i-v**). However, *pdat1* mutants displayed more leaf damage compared to wildtype after returning to growing conditions for two days. (**Fig. 2B, vi and C**). All acyltransferase mutants recovered, and after twelve days post-freezing they showed no changes in dry weight compared to wildtype (**Supplemental Fig. S7**).

Cellular electrolyte leakage reveals a disconnect between membrane integrity and TAG accumulation

After observing that both acyltransferase families participated in TAG production during the stepped low-temperature assay, but only loss of *pdat1* caused leaf damage, we decided to explore the link between TAG production and plasma membrane integrity using a faster low-temperature ramp (**Fig. 1C**) with paired measurements of electrolyte leakage (Willing and Leopold, 1983; Thalhammer et al., 2020). We reasoned that transient changes in TAG levels might have a more pronounced effect on cell damage when measured in a quickly changing environment, assuming that decreases in TAG represent transiently reductions in membrane remodeling and therefore transiently increased plasma membrane leakage. At -4.5°C, we measured TAG levels and found a decrease in *pdat1* (3.2%) and *pdat2* (2.9%) mutants, while all other mutants were similar to wild type (5.8%) (**Fig. 3A**). We hypothesized that decreases in TAG accumulation would directly correlate with impaired plasma membrane integrity. Therefore, we measured plasma membrane permeability and damage by assessing the electrical conductivity of ions leaked during decreasing temperatures. The inflection points on each curve were used to determine the LT_{50} value, which served as a proxy for the temperature at which 50% of the total electrolytes were released into solution. Results showed the LT_{50} for *dgat1* (-3.1°C), *dgat2* (-2.8°C), and *pdat2* (-2.6°C) occurred at significantly warmer temperatures compared to wild type (-4.1°C) (**Fig. 3B**). Also, *dgat1* and *dgat2* mutants reached their maximum leakages at warmer temperatures compared to wild type, which occurred at -10°C (**Fig. 3C**) (Warren et al., 1996). The leftward shift of the curve in the *dgat1* and *dgat2* mutants indicated a more damaged membrane (**Fig. 3C**).

Both DGATs and PDATs are necessary for high-temperature TAG production

To test the role of acyltransferase family members at high temperatures, we treated acyltransferase mutants at 37°C from zero to 300 minutes following the schematic in **Fig. 1D**. From zero to 200 minutes, TAG increased indistinguishably across all genotypes (**Fig. 4 A-C**). At 300 minutes there was statistically less TAG in *pdat1* (5.2%), *dgat2* (7.8%) and *dgat3* (7.3%) mutants, compared to wild type (11.6% of total fatty acids) (**Fig. 4D**). The *pdat1* decrease in TAG accumulation was approximately 45% and is in agreement with previous reports (Mueller et al., 2017). Throughout the challenge with high

temperatures, no phenotypic differences were observed in mutants compared to wild type (*data not shown*).

Loss of PDATs affects levels of phosphatidylcholine and free fatty acids during low temperatures

To investigate the role of PC as a direct substrate for the PDAT family, we measured PC levels during the stepped low-temperature assay for all mutants, as shown in **Fig. 5A**. For clarity, separate panels are dedicated to displaying data for *pdat1* and *pdat2* mutants, and TAG levels from all mutants (**Fig. 2A**) are displayed in **Fig. 5B**.

In wild type plants, PC levels spiked after one week at 4°C, decreased at two hours at -6°C, and then increased again at sixteen hours at -6°C (**Fig. 5A**). While most acyltransferase mutants followed this pattern, some deviated. After one week at 4°C, *pdat1* mutants had decreased levels of PC (6.5%) compared to wild type (16.7%), but their PC levels matched those of wild type after treatment with -6°C for two hours (**Fig. 5A**). In an opposite pattern, *pdat2* mutants had PC levels similar to wild type after one week at 4°C, but decreased after sixteen hours at -6°C (9.5%) compared to wild type (14.9%, **Fig. 5A**). The PC levels in *dgat2* and *dgat3* mutants also decreased somewhat after one week at 4°C (10.1%, and 9.9%, respectively), compared to wild type (**Supplemental Fig. S2**). While PC levels in *dgat2* mutants returned to wild type levels after 16 hours at -6°C, levels in *dgat3* mutants remained lower (**Supplemental Fig. S2**). The strongest changes in PC levels occurred in *pdat1* mutants and did not coincide with the strongest impairment of TAG levels, which occurred at the 16 hour time point (**Fig. 5B**) and coincided with leaf damage (**Fig. 2B,C**). We then considered the possibility that other substrates or byproducts of PDAT or DGAT may explain the coincidence of leaf damage and TAG level impairment. We quantified accumulation of lyso-PC, free fatty acids and DAG after treatment with -6°C for sixteen hours (**Supplemental Fig. S8**). Increases in lysolipids, free fatty acids, or DAG can damage membranes, as these are non-bilayer forming (Cevc and Richardsen, 1999). However, we observed no changes in lyso-PC or DAG levels, and there was a 4.6-fold decrease in free fatty acids in the *pdat1* mutant (0.5%) compared to wild type (2.3%).

Because plastid-derived fatty acids appear in TAG during temperature stress (Li-Beisson et al., 2010), we checked for changes in levels of the two most abundant plastid-derived lipids, MGDG and DGDG. Generally, MGDG levels remained constant until they decreased after sixteen hours at -6°C in both wild type and the acyltransferase mutants (**Fig. 5C**). The *dgat1* mutants began the assay with relatively higher

MGDG levels but returned to wild type levels after two days at 4°C. (**Supplemental Fig. S2**). The DGDG levels remained constant throughout the low-temperature assay, increasing only after sixteen hours at -6°C (**Supplemental Fig. S2**).

Loss of *pdat1* but not *dgat1* affects the accumulation of double bonds in TAG

Under normal conditions, TAG typically contains a relatively low number of double bonds. During temperature stress, the number of double bonds increases, often attributed to accumulation of fatty acids from membrane lipids due to membrane remodeling (Mueller et al., 2015; Tan et al., 2018). We quantified changes in TAG double bonds using a double bond index (DBI). Throughout the low-temperature step, the DBI of TAG steadily increased in wildtype (**Fig. 6A**) and all mutants (**Supplemental Fig. S3**). In *pdat1* mutants, the DBI of TAG increased less from the start of the assay (0.7) to 1.1 or 1.2 after two or 16 hours at -6°C, respectively (**Fig. 6A**). Notably, after 16 hours at -6°C, the DBI of *pdat1* TAG became distinguishably lower than wild type (2.0) (**Fig. 6A**).

Plastid lipids are characterized by higher ratios of 16C fatty acids, while lipids in other parts of the cell have higher ratios of 18C fatty acids (LaBrant et al., 2018). Despite the lower DBI of TAG from *pdat1* mutants after 16 hours at -6°C, the ratio of 16:3 to 18:3 fatty acids in TAG of *pdat1* mutants remained similar to that of the wild type. (**Fig. 6B**). This contrasts with that of *sfr2*, known to change the 16:3 to 18:3 ratio (Barnes et al., 2016).

To determine whether the reduced DBI observed in TAG was attributed to changes in PC, we also quantified the DBI of PC. Throughout the low-temperature regimen, the DBI in PC fluctuated slightly, but none of the acyltransferase mutants deviated significantly from wild type (**Fig. 6C**). The ratio of 16:3 to 18:3 in PC remained similar between the *pdat* mutants and the wild type, while the ratio in the *dgat2* mutants increased to 0.1 compared to wild type (0.08) (**Fig. 6D**). We also investigated the DBI of the major plastid membrane lipids MGDG and DGDG. While there were slight trends in the DBI over the course of the low-temperature regimen, no statistically significant changes were observed (**Supplemental Fig. S3**). When investigating any changes in DBI for lyso-PC, free fatty acids and DAG in the *pdat1* mutant, we found that only free fatty acids were more saturated than wild type plants (**Supplemental Fig. S8**).

Consistent with the observations in low temperatures, in high temperatures, all wildtype and mutant lines had an increasing trend in the DBI of TAG (**Fig. 6E**, **Supplemental Fig. S3**). Specifically, the wildtype

showed an increase in DBI from 0.4 at the start, to 1.0 after 200 minutes and 1.1 after 300 minutes. In the *pdat1* mutants, the DBI of TAG increased more gradually. It was measurably different from time zero after 300 minutes at 37°C (DBI increased from 0.29 to 0.55), but remained significantly lower than wildtype at 200 and 300 minutes (**Fig. 6E**). Additionally, in the TAG of *pdat1* mutants, there was a higher 16:3/18:3 ratio (0.3), compared to wild type (0.1) at 100 minutes (**Fig. 6F**). As the treatment at 37°C continued, the incorporation of 18:3 fatty acids into TAG increased more significantly than that of 16:3 (**Supplemental Fig. S6**), thus we chose to depict the 100-minute timepoint in **Fig. 6**.

We also examined any changes in the levels of fully saturated 16:0 and 18:0 fatty acids in the acyltransferase mutants during the high temperature. Generally, saturation levels decreased as time in heat progressed, except for *pdat1* mutants, which maintained higher saturation levels at 200 and at 300 minutes of 37°C treatment (0.8 and 0.7, respectively) compared to wild type (0.6 and 0.5, **Supplemental Fig. S3**). In the *pdat2* mutants, the TAG composition was more saturated (0.7) than wild type (0.5) at 300 minutes of 37°C (**Supplemental Fig. S3**).

Discussion

Previous studies described two TAG-producing acyltransferases as necessary for TAG accumulation during temperature stress. However, no studies examined mutants of all DGATs and PDATs. In this study, we aimed to investigate the requirement of all members of the two acyltransferase families responsible for TAG accumulation, and to take advantage of this system to explore the assumption that TAG accumulation is required for membrane integrity. We demonstrated that all five DGAT and PDAT family members are necessary for wildtype levels of TAG accumulation in low or high temperatures (**Figs. 2 and 4**), and that membrane integrity does not directly coincide with TAG accumulation (**Fig. 3**). Our results suggest that the severity and duration of temperature challenges influence the importance of specific acyltransferases, and that TAG accumulation may have a use in addition to being a lipid reservoir. Moreover, our results suggest that a more comprehensive understanding of the roles of multiple gene family members relevant to temperature tolerance can be obtained through the use of temperature regimens that vary length, onset, and severity of stress.

TAG is produced by multiple acyltransferases during temperature stress

In plants lacking DGAT1 or PDAT1 , decreases in TAG accumulation were correlated with decreased freezing tolerance, while overexpression lines were more tolerant than wild type (Arisz et al., 2018; Tan

et al., 2018; Demski et al., 2020). The periods of cold acclimation in these studies varied from two to four days at 4°C, followed by differing chilling (Demski et al., 2020) or freezing stresses (Arisz et al., 2018; Tan et al., 2018). In our study, we implemented a one-week cold acclimation period, as this is known to maximize freezing tolerance (Uemura et al., 1995) (**Fig. 1B**). When we measured TAG after one week at 4°C and after freezing, the *dgat1* levels were similar to wild type, which differed from what had been previously reported (Arisz et al., 2018; Tan et al., 2018). However, when we increased the sampling frequency and measured TAG after two days at 4°C, we found that *dgat1* mutants had less TAG than wild type, consistent with previous findings (**Fig. 2A**). We also expanded the known role of *pdat1* in chilling tolerance (Demski et al., 2020), to include a role in freezing tolerance and TAG accumulation during freezing (**Fig. 2A, C**) In high temperatures, impaired TAG accumulation has been associated with *pdat1* mutants (Mueller et al., 2015; Mueller et al., 2017). Our study supports this previous finding as we also observed 55% less TAG in *pdat1* mutants. By including the other acyltransferase family members, we showed that TAG levels also decreased in *dgat2* (by 33%) and *dgat3* (by 37%) mutants compared to wild type (**Fig. 4**).

To evaluate the functional significance of these observations, we measured freezing tolerance through two mechanisms: leaf damage after freezing, and recovery potential twelve days later. Leaf damage associated with insufficient freezing tolerance typically manifests within two days post-freezing (Wanner and Junttila, 1999), while recovery assessments based on meristematic activity and new leaf growth requires a longer timeframe (Minami et al., 2015; Saucedo-García et al., 2021). Interestingly, while the *pdat1* mutant showed leaf damage two days post-freezing, all acyltransferase mutants, including *pdat1,* had full recovery potential twelve days post-freezing (**Fig. 2B, C, Supplemental Fig. S7**). This suggests that TAG accumulation plays a role in early protection of leaf tissue after freezing (**Fig. 5**). It also suggests the role of TAG accumulation for meristem protection is minimal during the tested temperature regimens.

Exploring potential mechanisms underlying *pdat1* freezing sensitivity

Given the decreased TAG accumulation and observed leaf damage in *pdat1* mutants, we investigated the levels of potential acyl-transferase-derived toxic intermediates, DAG, lyso-PC, and free fatty acids. Interestingly, after 16 hours of freezing, we observed no changes in DAG or lyso-PC levels, and a surprising decrease in levels of free fatty acids (**Supplemental Fig. S8**). These findings suggest that the mechanisms controlling accumulation of these potentially toxic intermediates may be more robust than

those governing TAG accumulation. Therefore, the observed leaf damage in *pdat1* mutants is likely due to impaired membrane remodeling, rather than accumulation of toxic intermediates.

Disassociation of TAG accumulation and plasma membrane integrity in low temperatures

Production of TAG during temperature stress has been suggested to be a necessary byproduct of lipid remodeling to produce more tolerant membranes (Lu et al., 2020). Tan and colleagues found decreases in both plasma membrane integrity and TAG amounts for *dgat1* mutants (Tan et al., 2018). We found a similar decrease in membrane integrity for *dgat1* and *dgat2* mutants but without decreased TAG accumulation (**Fig. 3**). Conversely, *pdat1* mutants exhibited reduced TAG accumulation without compromised plasma membranes (**Fig. 3**). This apparent disconnect is not unprecedented. Warren et al., (1996) reported similar observations in *sfr2* and *sfr6* mutants (Warren et al., 1996). Notably, loss of either SFR2 (Moellering et al., 2010; Barnes et al., 2016) or SFR6 (Knight et al., 1999) causes membrane damage to chloroplasts, further suggesting that disruptions in internal membrane remodeling may be independent of plasma membrane integrity.

Taken together, these observations suggest that TAG accumulation and plasma membrane remodeling are not always coupled. This raises intriguing questions about the freezing sensitivity of the *pdat1* mutants (**Fig. 2**). It could be that *pdat1* is freezing sensitive due to internal membrane damage. Similarly, the loss of plasma membrane integrity in *dgat1* and *dgat2* mutants without changes in TAG levels remains unexplained. Our findings underscore the complex interplay between acyltransferases and their unique impact on membrane remodeling during low temperatures. The seemingly contradictory changes in TAG and plasma membrane integrity point towards potential alterations in TAG metabolism. Considering the pivotal role of plasma membrane remodeling in low-temperature tolerance (Willing and Leopold, 1983; Zhang et al., 2013), any impairments in the ability of lipids to be removed from the membrane, delaying remodeling could result in changes in integrity and leakage.

Acyl chain saturation of TAG during high and low-temperature stress is increased in the *pdat1* mutant

In the stepped low temperature assay, we found a decreased DBI in TAG of *pdat1* mutants (**Fig. 6A**) but we did not observe any changes in plastidic acyl chain flux via 16:3/18:3 ratios in TAG in any of the acyltransferase mutants (**Fig. 6B**), suggesting that plastid remodeling was not impaired. In high temperatures, *pdat1* mutants again showed a decreased DBI (**Fig. 6E**) and a corresponding increase in the saturation of TAG (**Supplemental Fig. S3**). Unlike during low temperatures, *pdat1* mutants did have a higher 16:3/18:3 ratio in the heat (**Fig. 6F**), which could indicate a lower 18:3 incorporation or a higher 16:3 incorporation into TAG. The PDAT1 enzyme has been reported to have a higher preference for 18:3

(Ståhl et al., 2004; Fan et al., 2013b) and its lack in the *pdat1* mutant may drive a relatively lower incorporation of 18:3 and higher 16:3/18:3 ratio. Alternatively, lipases specific to 18:3 may be impacted in the *pdat1* background. Lipases active in high temperatures and that control 18:3 release include HIL1 (Higashi et al., 2018), and PHOSPHOLIPASE A2 of *Chlamydomonas reinhardtii* (Légeret et al., 2016).

In both high and low temperature stress, polyunsaturated TAG was shown to accumulate in leaf tissue (Degenkolbe et al., 2012; Mueller et al., 2015; Shiva et al., 2020). Our results agree with these findings for wildtype Arabidopsis (**Fig. 6A, E**). However, in both our high and low-temperature assays, *pdat1* mutants showed a decreased DBI in TAG while all other mutants remained similar to wild type, suggesting *pdat1* mutants are unable to effectively remove polyunsaturated fatty acids into TAG (**Fig. 6A, E; Supplemental Fig. S3**). Again, this is consistent with the known preference of PDAT1 for 18:3 fatty acids (Ståhl et al., 2004; Fan et al., 2013b) and the absence of this activity in the *pdat1* mutants. Since acyl chain composition of membrane lipids and TAG were shown to be a crucial factor for temperature tolerance (Higashi and Saito, 2019), the altered DBI of the *pdat1* mutants could explain the impaired freezing recovery phenotype we observed (**Fig. 2**).

Major chloroplast lipids are not affected by acyltransferase mutants in low temperatures

Glycerolipids make up the largest fraction of membrane lipids and contribute to temperature tolerance via their relative ratios of head groups to one another. In the plastid, MGDG to DGDG ratios are essential to maintain the correct membrane curvature and organelle structure (Rocha et al., 2018; Yu et al., 2020). In both low and high temperatures, an increase in the lamellar lipid DGDG and a decrease in non-lamellar MGDG are observed, and imbalances lead to impaired plastid membrane integrity (Chen et al., 2006; Moellering et al., 2010; Zheng et al., 2016). Neither the MGDG and DGDG levels (**Fig. 5**), their DBI (**Supplemental Fig. S3**), nor their 16:3 to 18:3 ratios (**Supplemental Fig. S4**) were affected in the acyltransferase mutants. This suggests that the chloroplast was able to maintain relative levels of membrane lipids and saturation levels even while TAG accumulation was impaired (**Supplemental Fig. S3**), consistent with work showing that lipid synthesis not only occurs during low temperatures but is necessary for survival (Miquel et al., 1993; Li et al., 2004; Arisz et al., 2013; Barrero-Sicilia et al., 2017).

***pdat1* mutants alter PC amount and saturation in low-temperature stress.**

Just as MGDG and DGDG are the most abundant plastid lipids, PC is the most abundant extraplastidic membrane lipid. Its relative levels are critical to maintain membrane structure and function (Hamai et

al., 2006; Li et al., 2008; Ishiwata-Kimata et al., 2022). The PC levels were relatively lower in the *pdat1* mutants at 1 week of 4°C treatment but returned to wild-type levels at the end of the low-temperature step (**Fig. 5**). These changes to PC levels could have contributed to poor recovery of the *pdat1* mutants after freezing (**Fig. 2**). Inside the cell, PC is also a sink for lipid trafficking and many membrane lipid backbones are temporarily accumulated as PC prior to accumulation as TAG (Karki et al., 2019). We showed that PC levels had an overall DBI increase, consistent with remodeled lipids being incorporated into PC (**Fig. 6C**).

In conclusion, TAG accumulation in Arabidopsis during high and low temperatures is mediated by both DGAT and PDAT families. We show the severity and duration of temperature stress impact which acyltransferases are most critical for TAG production, and find that loss of any PDAT or DGAT family member shows a reduction in TAG in at least one condition. We also find the role of TAG accumulation is more complex than simply maintaining plasma membrane integrity. Taken together, this work highlights the importance of both acyltransferase families for TAG accumulation, plasma membrane integrity, and temperature tolerance.

Materials and Methods

Plant Materials

The Columbia ecotype of *Arabidopsis thaliana* was used for all wild-type samples. Homozygous T-DNA insertions for *dgat1* (SALK_039456C), *dgat2* (SALK_067809C), *dgat3* (GABI_696F08), *pdat1* (SALK_065334), *pdat2* (SALK_010854C), *mboat5* (SALK_021674C), and *sfr2-3* (SALK_106253) were confirmed using PCR with primers listed in (**Supplemental Table S1**). Acyl transferase mutants *dgat1, pdat1, and mboat5* were a kind gift from Dr. Timothy Durrett (Kansas State University). The remaining T-DNA mutants for the acyltransferase knockout lines were supplied from the Arabidopsis Biological Research Center. All lines are currently available from the Arabidopsis Biological Research Center.

Low-Temperature Step Assay and Recovery

Before planting, seeds were surface sterilized by washing in 30% bleach (8.25% sodium hypochlorite) for 28 minutes followed by five washes with sterile ddH_2O. Sterilized seeds were planted on solid ½ Murashige and Skoog with vitamins, no glycine media (Caisson Labs) containing 1% sucrose, 0.5% MES, and 0.6% Agargel (Sigma) at pH 5.7. Plated seeds were held at 4°C for two days in the dark and then

moved to the growth chamber (18-hour day/22°C, 120 μmol m^{-2} s^{-1} light; 6-hour night/18°C) for three weeks.

After three weeks of growth, plants were moved to a cold acclimation chamber held at 4°C (12-hour day/night, 60 μmol·m^{-2}·s^{-1} light) for 1 week. During cold acclimation, light intensity was decreased by half to prevent the induction of photoinhibition and high light stress (*reviewed in* Janda et al., 2014). Then, at the end of the relative day/night cycle plants were moved to a freezer (Darwin Chambers) without light at -2°C for two hours. After two hours, nucleation of ice formation was initiated by placing an ice chip on the media. Immediately following, the temperature was dropped to -6°C, and plants were held at this temperature for sixteen hours. While the chamber cools within 45 minutes to -6°C, the internal temperature of the agar plate reaches -6°C after seven hours as measured with a temperature logger (Lascar Electronics).

To assess leaf damage, the frozen plates were placed on a Styrofoam surface with less than 10 μmol·m^{-2}·s^{-1} (± 5%) of photosynthetically available light (Spectrum Technologies) for 24 hours where they gradually warmed to 21°C. After 24 hours, the plates were then moved back to the growth chamber for two day to assess leaf damage as described in (**Fig. 1B**, Moellering et al., 2010). Scoring of leaf damage was measured using a 1-3 scale, with 1 representing severe damage, 2 being partially damaged, and 3 showing no observable damage. Representative rosettes for each scoring class are shown in **Fig. 2B, vi**.

To assess whole plant recovery a modified assay from Minami et al was used (2015). Briefly, frozen plates were warmed on Styrofoam for 2.5 hours to 6°C and plants were transferred to chilled 8°C soil (Berger BM2 Seed Germination and Propagation Mix). To prevent shock from transferring, the plants were covered to prevent immediate high light stress and moved to a 10°C chamber for 24 hours. Plants were then moved to a growth chamber (22°C, 16 hour day/8 hour night) with a clear dome for two days. Following two days, the dome was removed, and plants were allowed to grow for a total of twelve days at which point post-freezing recovery was scored and biomass measurements were taken (**Supplemental Fig. S7**). For recovery scoring, a 1-3 scale was used with 1 being not able to recover, 2 being partially recovered, and 3 able to fully recover. Dry weight was measured on individual rosettes that has been allowed to dry in foil bags for four days at 65°C, $n \geq 60$ rosettes sampled over four growth trials.

Sampling

At each indicated point in **Fig. 1B**, a subset of plants was sampled for lipid analysis, and others were photographed. All samples were taken at the end of the respective day, except for freezing samples, which were taken the indicated numbers of hours post-end of day, and beginning of freezing. For lipid analysis, two rosettes were sampled in duplicate and immediately flash-frozen in liquid nitrogen and stored at -80°C until lipid extraction and analysis were performed. Each sample was considered one biological replicate Only rosette tissue was collected, roots were discarded. For quantification of low abundance lipids (free fatty acids (FFA), DAG, and lyso-phosphatidyl choline (Lyso-PC), four rosettes were sampled and lipids were immediately extracted as one biological replicate

For electrolyte leakage, two rosettes were harvested into a 5-mL snap cap tube containing 3-mL of 18.2 MΩ-cm resistance water. Duplicates were made for each temperature point. Each sample was considered one biological replicate.

For all experiments, there were a minimum of two growth trials conducted.

Lipid Extraction and Analysis

Lipids were extracted using the modified Bligh and Dyer method as described in (Mahboub et al., 2021). Thin-layer chromatography was then used to isolate lipids of interest. After extraction, lipids were dried down under N_2 gas, resuspended in an equal volume of chloroform, and loaded onto thin-layer chromatography plates pretreated with ammonium sulfate (Macherey-Nagel 810063). The first resolving solvent containing acetone: toluene: water (91:30:8, *v/v/v*) was run 12 cm from the loading site. The plate was then dried with N_2 and further resolved with a second solvent containing petroleum ether: diethyl ether: acetic (80:20:1 *v/v/v*).

For isolating FFA, DAG and Lyso-PC, dried lipids were resuspended in an equal volume of chloroform, and loaded onto Silica60 thin-layer chromatography plates (Sigma Aldrich 1.0521.0001). The first resolving solvent contained chloroform: methanol: acetic acid: acetone: water (35:25:4:14:2, *v/v/v/v/v*) was run 10 cm from the loading site, as described in (Xu et al., 1996). The plate was then dried with N_2 and further resolved with a second solvent containing petroleum ether: diethyl ether: acetic (80:20:1 *v/v/v*).

Silica bands containing lipids of interest were scraped, and pentadecanoic acid was added as an internal standard. Lipids were then derivatized into fatty acid methyl esters (FAMEs) as described in (Benning and Somerville, 1992). FAMEs were then separated using a 30-m HP-Innowax capillary column (Agilent) with hydrogen carrier gas. The separation method began at 90°C for one minute, ramped to 235°C at

30°C/min, was held at 235°C for five minutes, and ended with flame ionized detection. Outliers were first removed after analyzing the fatty acid composition of C16:3 and C18:3 for all mutants and wild type at each temperature tested using ROUT analysis at a 10% threshold (GraphPad v9.5.0) (Motulsky and Brown, 2006). Fatty acid profiles for lipids measured in the low- and high-temperature steps can be found in Supplemental Figures S5 and S6. Any outliers detected resulted in the removal of the lipid from further analysis. Following removal, relative mole percentages of MGDG, DGDG, PC, TAG, FFA, DAG, Lyso-PC were calculated as compared to the total lipids present. The resulting mole percents were then screened for outliers using one interquartile distance from the median for each lipid class of each genotype at each temperature. Asterisks indicate a significance of $P \leq 0.05$ calculated with Brown-Forsythe and Welch One-Way ANOVA compared to wild type control for MGDG, DGDG, PC, TAG. Asterisks indicate a significance of $P \leq 0.05$ calculated with an unpaired t test with Welch's correction for *pdat1* compared to wild type control.

Double bond index (DBI) was calculated using: $\frac{(X{:}1)\times 1+(X{:}2)\times 2+(X{:}3)\times 3}{100}$ where X represents the mole % of 16:n and 18:n fatty acids, where n is one, two, or three double bonds.

The saturation index was calculated in a similar way using: $\frac{16{:}0+18{:}0}{100}$.

Multiple comparisons were corrected by using Dunnett's test for comparisons to wild type directly, or Tukey's multiple comparisons test when genotypes were compared against one another. For all samples $n \geq 2$ growth trials each containing $n \geq 2$ replicates. (Ex. A minimum of four biological replicates grown in two separate growth trials).

<u>*Low-Temperature Ramp Assay and Electrolyte Leakage*</u>

To determine electrolyte leakage of the *Arabidopsis* at various subzero temperatures, a refrigerated chiller (AP15R, VWR) was used, and conditions were performed essentially as described in (Warren et al., 1996) chilling at a rate of 2°C/hour with slight modifications. Cellular leakage of electrolytes in the samples was measured using a conductivity meter (Orion Star A212, Thermo Scientific). Plants were grown as described in the *Low-Temperature Step Assay and Recovery* and were prepared as described in *Sampling*. The growth scheme and temperature profile used is diagramed in **Fig. 1C**, and representative images of rosettes following one week of cold acclimation are shown in **Fig 2B, iii**. Before application of low-temperature, conductivity was measured and recorded as initial leakage. Samples were then placed in floats to suspend in the refrigerated chiller set to 0°C and incubated for one hour. After one hour, ice formation was initiated using an ice chip (18-MΩ water) placed into the tube. Samples were then

collected from 0°C to -10°C and left to thaw overnight at 4°C. The chilling rate began at 3°C for samples collected above 0°C and no nucleation was used. The rate of cooling was the same as described. Conductivity was then measured and recorded as the leakage at the temperate when the sample was removed from the chiller. Finally, to measure the end-point leakage, samples were heated to 65°C for 30 minutes, cooled to room temperature, and then shaken at 250 rpm for fifteen minutes to release all electrolytes into solution. Conductivity was measured and recorded as final leakage.

Percent leakage was calculated using: $\frac{\text{Leakage at T(°C)}}{\text{Final Leakage} - \text{Average of Initial Leakage}} \times 100$

Percent leakage was normalized to zero using the initial leakage measurements, and outliers were removed with ROUT analysis set to 10%. The data was plotted along with a non-linear fit constrained to {x| 0 < x < 100} (GraphPad v9.5.0). Asymptotic 95% confidence interval was graphed for error, and LT_{50} values were recorded.

To compare data from the discontinuous freezing assay, lipids from wild type and the acyltransferase mutants were extracted from plants frozen to -4.5°C. Conditions for freezing with the refrigerated chiller and sample preparation were performed as described above. Once the internal temperature reached -4.5°C, samples were removed from the chiller and thawed at room temperature for 40 minutes. Rosettes were removed and blotted dry and immediately transferred into 1-mL of cold extraction buffer following the modified Bligh and Dyer described above. Lipids were then resolved using a ten-centimeter Silica-60 TLC plate (Sigma Aldrich 1.05721.0001) using a mobile phase containing petroleum ether: diethyl ether: acetic acid (80:20:1 *v/v/v*). Silica containing TAG was scraped derivatized into FAMEs, quantified and outliers removed as described in *Lipid Extraction and Analysis*.

High-Temperature Treatment

For high-temperature experiments, seeds (genotypes listed in *Plant Materials)* were surface sterilized in 70% ethanol with 0.05% Triton X-100 for fifteen minutes, followed by six washes with 95% ethanol and air-dried on sterile filter paper. Sterilized seeds were planted on solid ½ Murashige and Skoog media (Phytotech) that contained 1% sucrose and 0.5% phytagel (Sigma) at pH 5.7 for germination. Plated seeds were held at 4°C for three days in the dark and then moved to a growth chamber (18-hour day/22°C, 140 $\mu mol \cdot m^{-2} \cdot s^{-1}$ light; 6-hour night/18°C) for three days. After three days of incubation, seedlings were transferred to larger plates (media as described above) for fourteen days of growth.

Starting two hours after the start of their relative day, 17-day-old plants were subjected to non-lethal heat treatment at 37°C, as described in Mueller et al 2017 using a Liebherr incubator equipped with lamps at 140 $\mu mol \cdot m^{-2} \cdot s^{-1}$ illumination. Plates containing plants were placed into the incubator and were sampled after 0, 100, 200, and 300 minutes of heat treatment, as diagramed in **Fig. 1D**.

Sampling and Lipid Extraction During High-Temperature Treatment

After sampling rosette tissue, lipid extraction for the high-temperature treatment was immediately performed using the modified Shiva et al. (2018) method as described in (Mahboub et al., 2021). Rosette tissue was placed into one volume of isopropanol and boiled at 75°C for fifteen minutes. Three volumes of chloroform: methanol: water (30:41.5:3.5 *v/v/v*) were then added and samples were incubated at 37°C on an orbital shaker at 250 rpm for 24 hours. The plant tissue was then removed and the solvent was evaporated under nitrogen gas. Dried lipids were stored at -20°C. $n \geq 2$ growth trials each containing $n \geq 2$ biological replicates. (Ex. A minimum of four biological replicates grown in two separate growth trials)

Lipid Analysis During High-Temperature Treatment

Dried lipids were resuspended in chloroform. An equal volume of resuspended lipids was loaded onto TLC plates (SIL G, Macherey-Nagel) for TAG separation and total fatty acid analysis. Plates were placed into tanks containing petroleum ether: diethyl ether: acetic acid (80:20:1 *v/v/v*). Silica bands containing lipids of interest were scraped, derivatized, and standardized as described in (Benning and Somerville, 1992). Samples were separated using a 30 m capillary DB-23 column (Agilent) with helium carrier gas. The separation method began at 90°C for 1 min, ramped to 235°C at 30°C min^{-1}, was held at 235°C for 5 min, and ended with detection flame ionization. Data analysis was completed as described in *Lipid Extraction and Analysis*.

Author contributions

ZDS, RLR, and JW designed the research; ZDS, SM, HV, and JW performed research; TT contributed analytic tools; ZDS analyzed the data and wrote the manuscript; all authors edited the article.

Supplemental Data

Supplemental Figure S1: Relative mole percents of MGDG, DGDG, and PC following the low-temperature step.

Supplemental Figure S2: Line graphs of the relative mole percents of MGDG, DGDG, PC, and TAG in low-temperature step. Supplemental Fig. S3: Double bond and saturation index for TAG, MGDG, DGDG, and PC for both the low- and high-temperature steps.

Supplemental Figure S4: 16:3/18:3 ratios for TAG, MGDG, DGDG, and PC during the low- and high-temperature steps.

Supplemental Figure S5: Relative mole percent of fatty acids for TAG, MGDG, and DGDG following the low-temperature step.

Supplemental Figure S6: Relative mole percent of fatty acids for PC in the low-temperature step and TAG in the high-temperature step.

Supplemental Fig. S7: All acyltransferase mutants are able to recover after a 12-day period.

Supplemental Fig. S8: Relative mole percents, doiuble bond, and saturation indicies for lyso-PC, DAG, and free fatty acids after sixteen hours of freezing.

Supplemental Table S1: Primers used for genotyping loss-of-function mutants

Supplemental Table S2: Average Scoring Percents of Leaf Damage Two Days Post-Freezing

Acknowledgements

We would like to thank Aline Rodrigues de Queiroz, Evan LaBrant, and Cailin Smith for their thoughtful feedback on this work.

Funding

This work was supported by the National Science Foundation (IOS-1845175), and partially supported by the Nebraska Agricultural Experiment Station with funding from the Hatch Multistate Research capacity funding program (Accession Number NC1203) from the USDA National Institute of Food and Agriculture. JW was supported by the Kasetsart University Research and Development Institute, KURDI (FF(KU)22.64) and the National Science and Technology Development Agency (FDA-CO-2561-8404-TH).

References

Arisz SA, Heo J-Y, Koevoets IT, Zhao T, van Egmond P, Meyer AJ, Zeng W, Niu X, Wang B, Mitchell-Olds T, et al DIACYLGLYCEROL ACYLTRANSFERASE1 Contributes to Freezing Tolerance. *Plant Physiol.* 2018:**177**:1410–1424. https://doi.org/10.1104/pp.18.00503

Arisz SA, van Wijk R, Roels W, Zhu J-K, Haring MA, Munnik T (2013) Rapid phosphatidic acid accumulation in response to low temperature stress in Arabidopsis is generated through diacylglycerol kinase. *Front Plant Sci.* 2013:**4**:1-15 https://doi.org/10.3389/fpls.2013.00001

Aymé L, Arragain S, Canonge M, Baud S, Touati N, Bimai O, Jagic F, Louis-Mondésir C, Briozzo P, Fontecave M, et al Arabidopsis thaliana DGAT3 is a [2Fe-2S] protein involved in TAG biosynthesis. *Sci Reports* 2018:**8**:1–10. https://doi.org/10.1038/s41598-018-35545-7

Bao X, Focke M, Pollard M, Ohlrogge J Understanding *in vivo* carbon precursor supply for fatty acid synthesis in leaf tissue. *Plant J.* 2000:**22**:39–50. https://doi.org/10.1046/j.1365-313x.2000.00712.x

Barnes AC, Benning C, Roston RL Chloroplast Membrane Remodeling during Freezing Stress Is Accompanied by Cytoplasmic Acidification Activating SENSITIVE TO FREEZING2. *Plant Physiol.* 2016:**171**:2140–2149. https://doi.org/10.1104/pp.16.00286

Barnes AC, Myers JL, Surber SM, Liang Z, Mower JP, Schnable JC, Roston RL Oligogalactolipid production during cold challenge is conserved in early diverging lineages. *J Exp Bot.* 2023:**17**:5405-5417. https://doi.org/10.1093/jxb/erad241

Barrero-Sicilia C, Silvestre S, Haslam RP, Michaelson L V. Lipid remodelling: Unravelling the response to cold stress in Arabidopsis and its extremophile relative *Eutrema salsugineum*. *Plant Sci* 2017:**263**: 194-200. https://doi.org/10.1016/j.plantsci.2017.07.017

Benning C, Somerville CR Isolation and genetic complementation of a sulfolipid-deficient mutant of *Rhodobacter sphaeroides*. *J Bacteriol* 1992:**174**:2352–2360. https://doi.org/10.1128/jb.174.7.2352-2360.1992

Burke M, Emerick K Adaptation to Climate Change: Evidence from US Agriculture. *Am Econ J Econ Policy* 2016:**8**:106–140. https://doi.org/ 10.1257/pol.20130025

Carro M de las M, Gonorazky G, Soto D, Mamone L, Bagnato C, Pagnussat LA, Beligni MV Expression of *Chlamydomonas reinhardtii* chloroplast DIACYLGLYCEROL ACYLTRANSFERASE3 is induced by light in concert with triacylglycerol accumulation. *Plant J* 2022:**110**:262–276. https://doi.org/10.1111/tpj.15671

Cevc G, Richardsen H Lipid vesicles and membrane fusion. *Adv Drug Deliv Rev* 1999:**38**: 207–232. https://doi.org/10.1016/S0169-409X(99)00030-7

Chen J, Burke JJ, Xin Z, Xu C, Velten J Characterization of the Arabidopsis thermosensitive mutant *atts02* reveals an important role for galactolipids in thermotolerance. *Plant Cell Environ* 2006:**29**:1437–1448. https://doi.org/10.1111/j.1365-3040.2006.01527.x

Cohen J, Agel L, Barlow M, Garfinkel CI, White I Linking Arctic variability and change with extreme winter weather in the United States. *Science* 2021:**373**:1116–1121. https://doi.org/10.1126/science.abi9167

Degenkolbe T, Giavalisco P, Zuther E, Seiwert B, Hincha DK, Willmitzer L Differential remodeling of the

lipidome during cold acclimation in natural accessions of *Arabidopsis thaliana*. *Plant J* 2012:**72**: 972–982. https://doi.org/10.1111/tpj.12007

Demski K, Łosiewska A, Jasieniecka-Gazarkiewicz K, Klińska S, Banaś A PHOSPHOLIPID:DIACYLGLYCEROL ACYLTRANSFERASE1 Overexpression Delays Senescence and Enhances Post-heat and Cold Exposure Fitness. *Front Plant Sci*. 2020:**11**:1–14. https://doi.org/10.3389/fpls.2020.611897

Du Z-Y, Lucker BF, ZIENKIEWICZ K, Miller TE, Zienkiewicz A, Sears BB, Kramer DM, Benning C Galactoglycerolipid Lipase PGD1 Is Involved in Thylakoid Membrane Remodeling in Response to Adverse Environmental Conditions in Chlamydomonas. *Plant Cell* 2018:**30**: 447–465. https://doi.org/10.1105/tpc.17.00446

Falcone DL, Ogas JP, Somerville CR Regulation of membrane fatty acid composition by temperature in mutants of Arabidopsis with alterations in membrane lipid composition. *BMC Plant Biol*. 2004:**4**:17. https://doi.org/10.1186/1471-2229-4-17

Fan J, Yan C, Xu C PHOSPHOLIPID:DIACYLGLYCEROL ACYLTRANSFERASE-mediated triacylglycerol biosynthesis is crucial for protection against fatty acid-induced cell death in growing tissues of Arabidopsis. *Plant J*. 2013a:**76**:930–942. https://doi.org/10.1111/tpj.12343

Fan J, Yan C, Zhang X, Xu C Dual role for PHOSPHOLIPID:DIACYLGLYCEROL ACYLTRANSFERASE: enhancing fatty acid synthesis and diverting fatty acids from membrane lipids to triacylglycerol in arabidopsis leaves. *Plant Cell* 2013b:**25**:3506–3518. https://doi.org/10.1105/tpc.113.117358

Ghosh UK, Islam MN, Siddiqui MN, Khan MAR Understanding the roles of osmolytes for acclimatizing plants to changing environment: a review of potential mechanism. *Plant Signal Behav*. 2021:**16**:1-13. https://doi.org/10.1080/15592324.2021.1913306

Gilmour SJ, Hajela RK, Thomashow MF Cold Acclimation in *Arabidopsis thaliana*. *Plant Physiol* 1988:**87**:745–750. https://doi.org/10.1104/pp.87.3.745

Guihur A, Rebeaud ME, Goloubinoff P How do plants feel the heat and survive? T*rends Biochem Sci* 2022:**47**:824–838. https://doi.org/10.1016/j.tibs.2022.05.004

Gusta L V., Wisniewski ME, Trischuk RG Patterns of freezing in plants: the influence of species, environment and experiential procedures. Plant cold hardiness from Lab. to F. CABI, UK 2009:214–225. http://dx.doi.org/10.1079/9781845935139.0214

Hamai C, Yang T, Kataoka S, Cremer PS, Musser SM Effect of average phospholipid curvature on supported bilayer formation on glass by vesicle fusion. *Biophys J* 2006:**90**:1241–1248. https://doi.org/10.1529/biophysj.105.069435

Higashi Y, Okazaki Y, Takano K, Myouga F, Shinozaki K, Knoch E, Fukushima A, Saito K HEAT INDUCIBLE LIPASE1 remodels chloroplastic monogalactosyldiacylglycerol by liberating α-linolenic acid in Arabidopsis leaves under heat stress. *Plant Cell* 2018:**30**:1887–1905. https://doi.org/10.1105/tpc.18.00347

Higashi Y, Saito K Lipidomic studies of membrane glycerolipids in plant leaves under heat stress. *Prog Lipid Res* 2019:**75**:1-14. https://doi.org/10.1016/j.plipres.2019.100990

Ishiwata-Kimata Y, Le QG, Kimata Y Induction and aggravation of the endoplasmic-reticulum stress by membrane-lipid metabolic intermediate phosphatidyl-*N*-monomethylethanolamine. *Front Cell Dev Biol*. 2022:**9**:1-11. https://doi.org/10.3389/fcell.2021.743018

Janda T, Majláth I, Szalai G Interaction of Temperature and Light in the Development of Freezing Tolerance in Plants. *J Plant Growth Regul*. 2014:**33**:460–469. https://doi.org/10.1007/s00344-013-9381-1

Karki N, Johnson BS, Bates PD Metabolically distinct pools of phosphatidylcholine are involved in trafficking of fatty acids out of and into the chloroplast for membrane production. *Plant Cell* 2019:**11**:2768-2788. https://doi.org/10.1105/tpc.19.00121

Klypina N, Hanson SF *Arabidopsis thaliana* wax synthase gene homologues show diverse expression patterns that suggest a specialized role for these genes in reproductive organs. *Plant Sci* 2008:**175**:312–320. https://doi.org/10.1016/j.plantsci.2008.05.002

Knight H, Veale EL, Warren GJ, Knight MR The *sfr6* mutation in Arabidopsis suppresses low-temperature induction of genes dependent on the CRT/DRE sequence motif. *Plant Cell* 1999:**11**:875–886. https://doi.org/10.1105/tpc.11.5.875

LaBrant E, Barnes AC, Roston RL Lipid transport required to make lipids of photosynthetic membranes. *Photosynth Res* 2018:**138**:345–360. https://doi.org/10.1007/s11120-018-0545-5

Légeret B, Schulz-Raffelt M, Nguyen HM, Auroy P, Beisson F, Peltier G, Blanc G, Li-Beisson Y Lipidomic and transcriptomic analyses of *Chlamydomonas reinhardtii* under heat stress unveil a direct route for the conversion of membrane lipids into storage lipids. *Plant Cell Environ* 2016:**39**:834–847. https://doi.org/10.1111/pce.12656

Li-Beisson Y, Shorrosh B, Beisson F, Andersson MX, Arondel V, Bates PD, Baud S, Bird D, DeBono A, Durrett TP, et al Acyl-Lipid Metabolism. *Arab B* 2010:**8**:1-65. https://doi.org/10.1199/tab.0133

Li-Beisson Y, Beisson F, Riekhof W Metabolism of acyl-lipids in *Chlamydomonas reinhardtii*. *Plant J* 2015:**82**:504–522. https://doi.org/10.1111/tpj.12787

Li W, Li M, Zhang W, Welti R, Wang X The plasma membrane–bound phospholipase Dδ enhances

freezing tolerance in *Arabidopsis thaliana*. *Nat Biotechnol* 2004:**22**: 427–433 https://doi.org/10.1038/nbt949

Li W, Wang R, Li M, Li L, Wang C, Welti R, Wang X Differential degradation of extraplastidic and plastidic lipids during freezing and post-freezing recovery in *Arabidopsis thaliana*. *J Biol Chem* 2008:**283**:461–468. https://doi.org/10.1074/jbc.m706692200

Lindquist S The Heat-Shock Response. *Annu Rev Biochem* 1986:**55**:1151–1191. https://doi.org/10.1146/annurev.bi.55.070186.005443

Liu Q, Siloto RMP, Lehner R, Stone SJ, Weselake RJ ACYL-CoA:DIACYLGLYCEROL ACYLTRANSFERASE: Molecular biology, biochemistry and biotechnology. *Prog Lipid Res* 2012:**51**:350–377. https://doi.org/10.1016/j.plipres.2012.06.001

Lu J, Xu Y, Wang J, Singer SD, Chen G The role of triacylglycerol in plant stress response. *Plants*. 2020:**9**:1-13. https://doi.org/10.3390/plants9040472

Mahboub S, Shomo ZD, Regester RM, Albusharif M, Roston RL Three methods to extract membrane glycerolipids: comparing sensitivity to lipase degradation and yield. *Methods Mol Bio* 2021:**2295**:15–27. https://doi.org/10.1007/978-1-0716-1362-7_2

Mhaske V, Beldjilali K, Ohlrogge J, Pollard M Isolation and characterization of an Arabidopsis thaliana knockout line for PHOSPHOLIPID: DIACYLGLYCEROL TRANSACYLASE gene (At5g13640). *Plant Physiol Biochem* 2005:**43**:413–417. https://doi.org/10.1016/j.plaphy.2005.01.013

Minami A, Tominaga Y, Furuto A, Kondo M, Kawamura Y, Uemura M Arabidopsis dynamin-related protein 1E in sphingolipid-enriched plasma membrane domains is associated with the development of freezing tolerance. *Plant J.* 2015:**83**:501–514. https://doi.org/10.1111/tpj.12907

Miquel M, James D, Dooner H, Browse J Arabidopsis requires polyunsaturated lipids for low-temperature survival. *Proc Natl Acad Sci.* 1993:**90**:6208–6212. https://doi.org/10.1073/pnas.90.13.6208

Moellering ER, Muthan B, Benning C Freezing tolerance in plants requires lipid remodeling at the outer chloroplast membrane. *Science* 2010:**330**:226–228. https://doi.org/10.1126/science.1191803

Motulsky HJ, Brown RE Detecting outliers when fitting data with nonlinear regression – a new method based on robust nonlinear regression and the false discovery rate. *BMC Bioinformatics* 2006:**7**:123. https://doi.org/10.1186/1471-2105-7-123

Mueller SP, Krause DM, Mueller MJ, Fekete A Accumulation of extra-chloroplastic triacylglycerols in Arabidopsis seedlings during heat acclimation. *J Exp Bot* 2015:**66**:4517–4526. https://doi.org/10.1093/jxb/erv226

Mueller SP, Unger M, Guender L, Fekete A, Mueller MJ PHOSPHOLIPID:DIACYLGLYCEROL ACYLTRANSFERASE-mediated triacylglyerol synthesis augments basal thermotolerance. *Plant Physiol* 2017:**175**:486–497. https://doi.org/10.1104/pp.17.00861

Rocha J, Nitenberg M, Girard-Egrot A, Jouhet J, Maréchal E, Block MA, Breton C Do galactolipid synthases play a key role in the biogenesis of chloroplast membranes of higher plants? *Front Plant Sci* 2018:**9**:1-7. https://doi.org/10.3389/fpls.2018.00126

Saha S, Enugutti B, Rajakumari S, Rajasekharan R Cytosolic triacylglycerol biosynthetic pathway in oilseeds. Molecular cloning and expression of peanut cytosolic diacylglycerol acyltransferase. *Plant Physiol* 2006:**141**:1533–1543. https://doi.org/10.1104/pp.106.082198

Saucedo-García M, González-Córdova CD, Ponce-Pineda IG, Cano-Ramírez D, Romero-Colín FM, Arroyo-Pérez EE, King-Díaz B, Zavafer A, Gavilanes-Ruíz M Effects of MPK3 and MPK6 kinases on the chloroplast architecture and function induced by cold acclimation in Arabidopsis. *Photosynth Res* 2021:**149**:201–212. https://doi.org/10.1007/s11120-021-00852-0

Schmid-Siegert E, Stepushenko O, Glauser G, Farmer EE Membranes as structural antioxidants: recycling of malondialdehyde to its source in oxidation-sensitive chloroplast fatty acids. *J Biol Chem* 2016:**291**:13005–13013. https://doi.org/10.1074/jbc.m116.729921

Shiva S, Samarakoon T, Lowe KA, Roach C, Vu HS, Colter M, Porras H, Hwang C, Roth MR, Tamura P, et al. Leaf lipid alterations in response to heat stress of *Arabidopsis thaliana*. *Plants* 2020:**9**:1-22. https://doi.org/10.3390/plants9070845

Shockey JM, Gidda SK, Chapital DC, Kuan J-C, Dhanoa PK, Bland JM, Rothstein SJ, Mullen RT, Dyer JM Tung tree DGAT1 and DGAT2 have nonredundant functions in triacylglycerol biosynthesis and are localized to different subdomains of the endoplasmic reticulum. *Plant Cell* 2006:**18**:2294–2313. https://doi.org/10.1105/tpc.106.043695

Ståhl U, Carlsson AS, Lenman M, Dahlqvist A, Huang B, Banaś W, Banaś A, Stymne S Cloning and functional characterization of a PHOSPHOLIPID:DIACYLGLYCEROL ACYLTRANSFERASE from Arabidopsis. *Plant Physiol* 2004:**135**:1324–1335 https://doi.org/10.1105/tpc.106.043695

Tan W-J, Yang Y-C, Zhou Y, Huang L-P, Xu L, Chen Q-F, Yu L-J, Xiao S DIACYLGLYCEROL ACYLTRANSFERASE and DIACYLGLYCEROL KINASE modulate triacylglycerol and phosphatidic acid production in the plant response to freezing stress. *Plant Physiol* 2018:**177**:1303–1318. https://doi.org/10.1104/pp.18.00402

Thalhammer A, Pagter M, Hincha DK, Zuther E Measuring Freezing Tolerance of Leaves and Rosettes: Electrolyte Leakage and Chlorophyll Fluorescence Assays. *Methods Mol Biol* 2020:**2156**: 9–21.

https://doi.org/10.1007/978-1-0716-0660-5_2

Uemura M, Joseph RA, Steponkus PL Cold acclimation of *Arabidopsis thaliana* (effect on plasma membrane lipid composition and freeze-induced lesions). *Plant Physiol* 1995:**109**:15–30. https://doi.org/10.1104/pp.109.1.15

Wang T, Xing J, Liu X, Yao Y, Hu Z, Peng H, Xin M, Zhou D-X, Zhang Y, Ni Z GCN5 contributes to stem cuticular wax biosynthesis by histone acetylation of CER3 in Arabidopsis. *J Exp Bo*t 2018:**69**:2911–2922. https://doi.org/10.1093/jxb/ery077

Wanner LA, Junttila O (1999) Cold-induced freezing tolerance in Arabidopsis. *Plant Physiol* **120**: 391–400 https://doi.org/10.1104/pp.120.2.391

Warren G, McKown R, Marin A, Teutonico R Isolation of mutations affecting the development of freezing tolerance in *Arabidopsis thaliana (L.) Heynh*. *Plant Physiol* 1996:**111**:1011–1019. https://doi.org/10.1104/pp.111.4.1011

Willing RP, Leopold AC Cellular Expansion at Low Temperature as a Cause of Membrane Lesions. *Plant Physiol.* 1983:**71**: 118–121 https://doi.org/10.1104/pp.71.1.118

Xu G, Waki H, Kon K, Ando S Thin-layer chromatography of phospholipids and their lyso forms: application to determination of extracts from rat hippocampal CA1 region. *Microchem J* 1996:**53**:29–33. https://doi.org/10.1006/mchj.1996.0005

Yu CW, Lin YT, Li H-min Increased ratio of galactolipid MGDG:DGDG induces jasmonic acid overproduction and changes chloroplast shape. *New Phytol* 2020:**228**:1327–1335. https://doi.org/10.1111/nph.16766

Yu L, Fan J, Zhou C, Xu C Chloroplast lipid biosynthesis is fine-tuned to thylakoid membrane remodeling during light acclimation. *Plant Physiol* 2021:**185**:94–107. https://doi.org/10.1093/plphys/kiaa013

Zhang XD, Wang RP, Zhang FJ, Tao FQ, Li WQ Lipid profiling and tolerance to low-temperature stress in *Thellungiella salsuginea* in comparison with *Arabidopsis thaliana*. *Biol Plant* 2013:**57**: 149–153 https://doi.org/10.1007/s10535-012-0137-8

Zheng G, Li L, Li W Glycerolipidome responses to freezing- and chilling-induced injuries: Examples in Arabidopsis and rice. BMC Plant Biol 2016:**16**:1–15. https://doi.org/10.1186%2Fs12870-016-0758-8

Author Notes

Rebecca Roston and Jaruswan Warakanont contributed equally to this work.

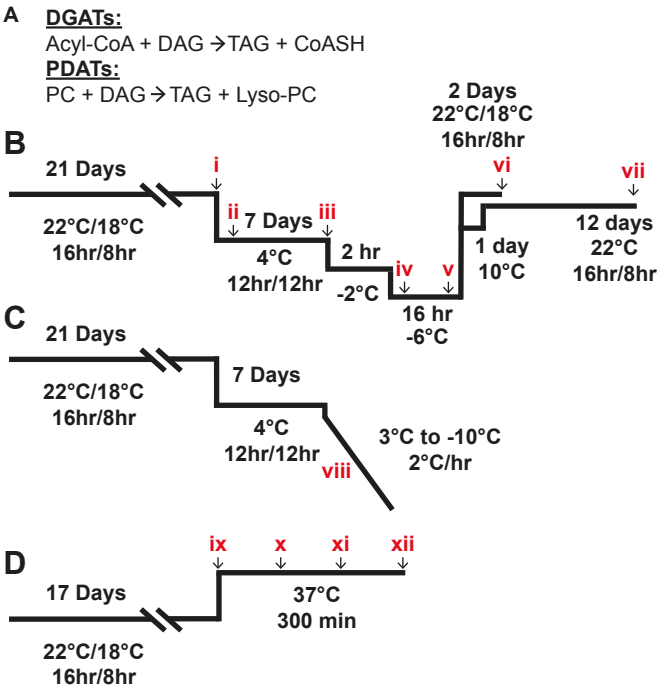

Fig. 1: Low and High-Temperature Treatment Regimens
(**A**) Enzymatic reaction of the DGAT and PDAT enzymes highlighting the differences in substrates and products. (**B**) Schematic of the low-temperature step used for lipid analysis and phenotyping. Red Roman numerals indicate sampling after 3 weeks of growth (i), 2 days into cold acclimation at 4°C (ii), 1 week of cold acclimation at 4°C (iii), 2 hours into freezing at -6°C (iv), 16 hours of freezing at -6°C (v), 2 (vi) or 12 (vii) days post-freezing at growing conditions. Line for 22°C recovery after 12 days (vii) is offset for ease of viewing. (**C**) Schematic of growth, cold acclimation, and low-temperature ramp starting at 3°C and dropping to -10°C over the course of 8 hours to assess membrane integrity (viii). (**D**) Schematic of the high-temperature step applied after seventeen days of growth. Sampling was at 0 minutes (ix), 100 minutes (x), 200 minutes (xi),

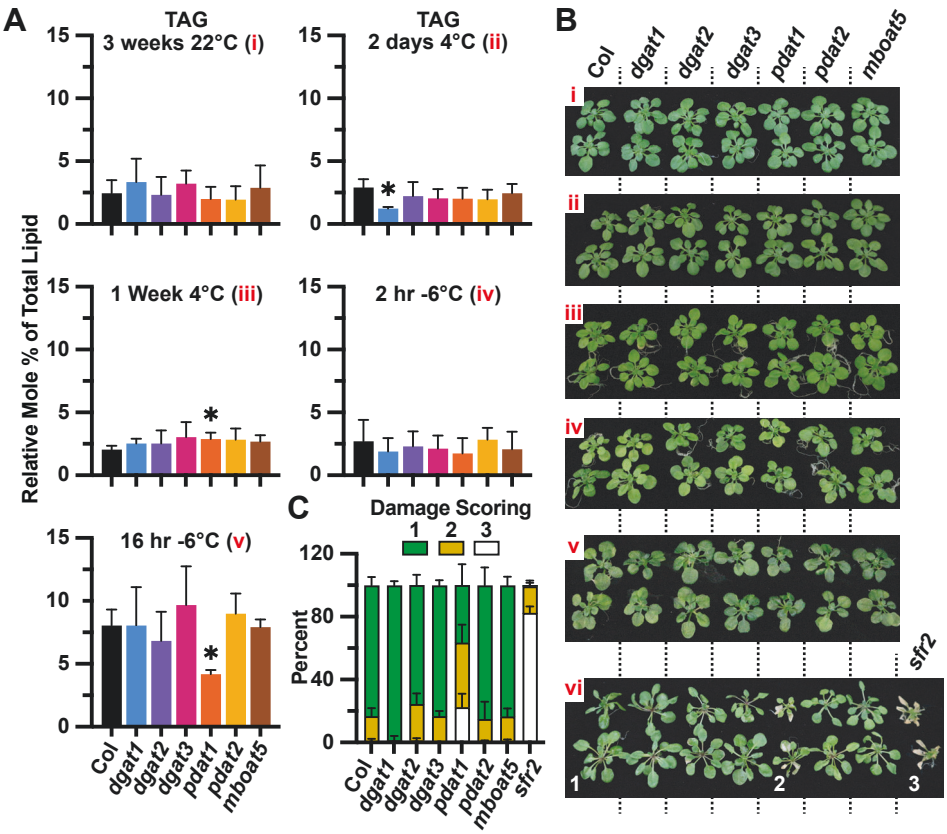

Fig. 2: *dgat1* and *pdat1* mutants uniquely affect TAG accumulation and leaf damage during the low-temperature step. (**A**) Relative mole percents of TAG analyzed following the treatment in **Fig. 1B** denoted with Roman numerals. n ≥ 4 biological replicates. Error bars show standard deviations, and asterisks show significance of $P \leq 0.05$ using Brown-Forsythe and Welch one-way ANOVA compared to wild type control. (**B**) Photographs of representative rosettes taken at each temperature sampled; Roman numerals correspond to the schematic in **Fig. 1B**. (**C**) Quantification of leaf damage in **Fig. 2B, vi** after two days of regrowth based on manual scoring. Representative rosettes given each score of 1, 2, or 3 are labeled in **Fig. 2B, vi**. Percents used can be found in **Supplemental Table S2**. n ≥ 74 rosettes. Error bars show standard deviations, and asterisks show significance of $P \leq 0.05$ using two-way ANOVA compared to wildtype control. Corresponding levels of MGDG, DGDG, and PC can be found in **Fig. S1**.

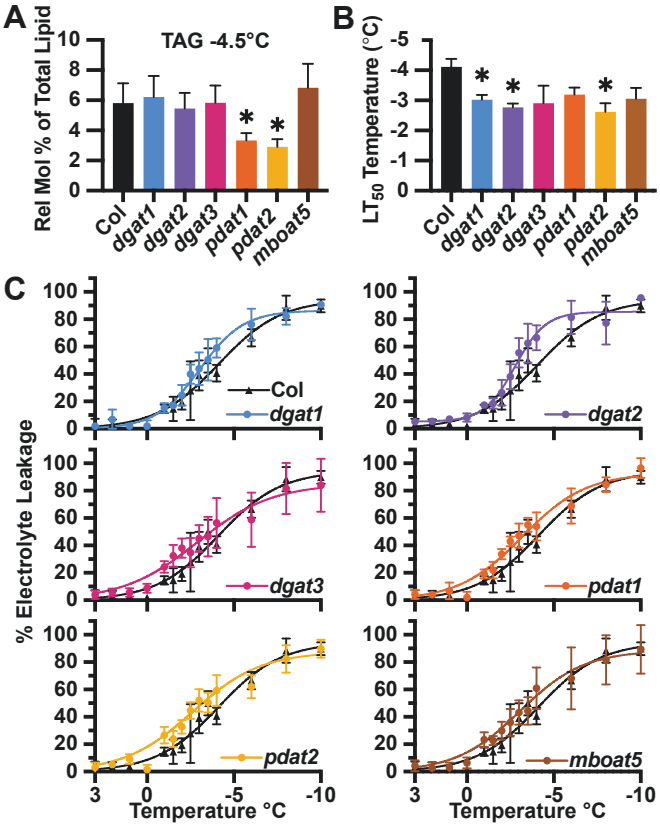

Fig. 3: Plasma membrane integrity and TAG accumulation are not linked in the acyltransferase mutants. (**A**) TAG levels quantified at -4.5°C using the assay in **Fig. 1C**. n ≥ 16 biological replicates. Error bars depict SD, and significance denoted with an asterisk for $P \leq 0.05$ using Brown-Foyrsythe and Welch one-way ANOVA. (**B**) LT_{50} temperatures from the full data shown in (**C**). Error bars depict SD, and significance denoted with an asterisk for $P \leq 0.05$ using Brown-Foyrsythe and Welch one-way ANOVA. (**C**) Cellular electrolyte leakage of acyltransferase mutants measured from 3°C to -10°C, compared to wild type control (**Fig. 1C**). Error bars depict 95% CI. n ≥ 6 biological replicates.

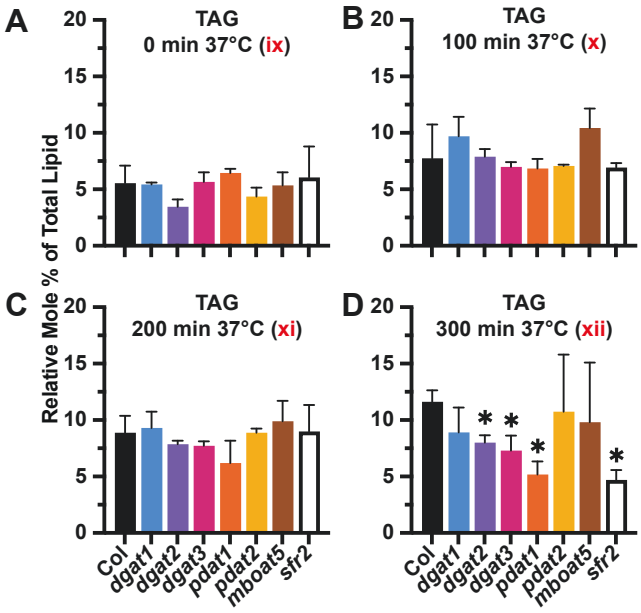

Fig. 4: Both families of acyltransferase mutants show reduced TAG accumulation in response to heat challenge. Relative mole percent of TAG from Arabidopsis challenged with a 37°C heat stress for 0 minutes (**A**), 100 minutes (**B**), 200 minutes (**C**), and 300 minutes (**D**). Treatment and Roman numerals correspond to **Fig. 1D**. Error bars represent standard deviations, and asterisks indicate significance of $P \leq 0.05$ calculated with Brown-Forsythe and Welch one-way ANOVA compared to wild type control. n ≥ 4 biological replicates.

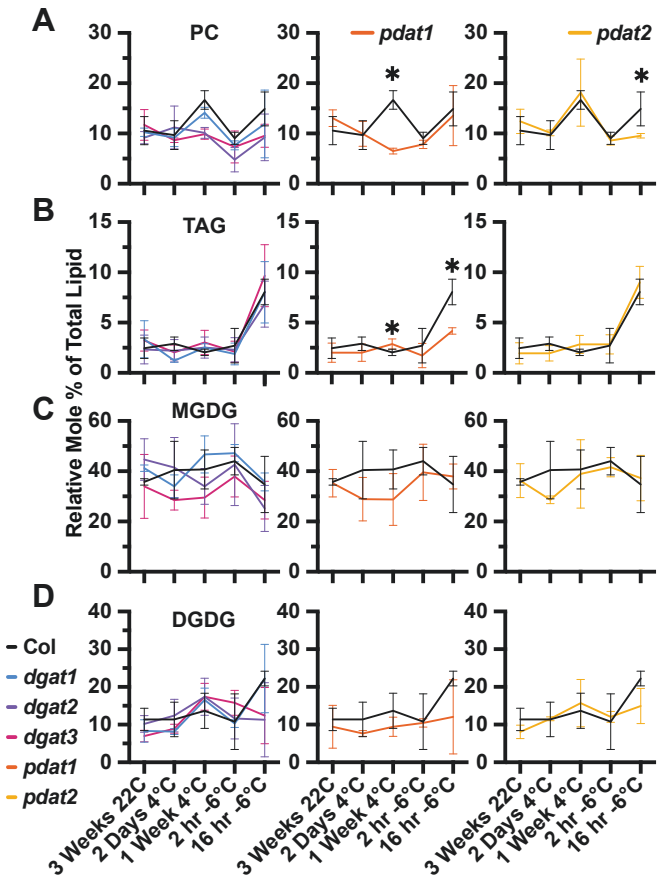

Fig. 5: Loss of PDATs affect the levels of PC when challenged with low temperatures. Line graphs depicting the changes in levels of PC (**A**), TAG (**B**), MGDG (**C**), and DGDG (**D**) during the low-temperature step (**Fig. 1B**). All mutants along with wild type are overlaid at the left of each panel, with *pdat1* and *pdat2* shown to the right for each lipid class respectively. n ≥ 4 biological replicates. Error bars represent standard deviations, and asterisks indicate significance of $P \leq 0.05$ calculated with Brown-Forsythe and Welch one-way ANOVA of the mutant compared to wild type control. Full data can be found in **Fig. S2**.

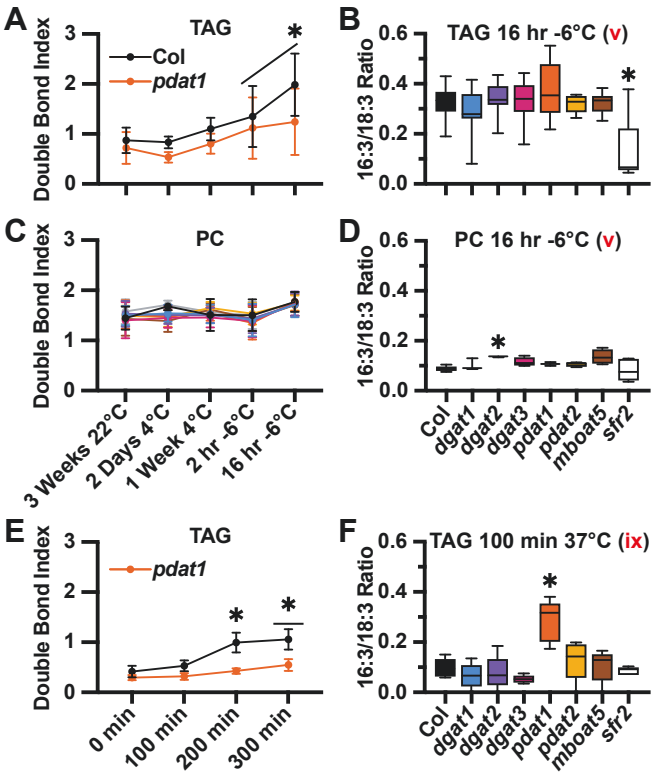

Fig. 6: *pdat1* mutants affect unsaturation in TAG in low and high-temperature treatments. DBI for TAG in *pdat1* mutants (**A**, **E**) and PC (**C**) in the low- or high-temperature step. Selected 16:3/18:3 ratios at 16 hours of -6°C TAG (**B**), or PC (**D**) and at 100 min of 37°C (**F**). Lines above the data points in (**A**) and (**E**) denote significance at that time point against itself at the start of the assay at 3 weeks 22°C (**A**), or 0 min 37°C (**E**). Asterisks denote significance to Col at the time point indicated. n ≥ 4 biological replicates. Error bars represent standard deviations, and all asterisks indicate significance of $P \leq 0.05$ calculated with Brown-Forsythe and Welch one-way ANOVA (**B**, **D**, and **F**) or a two-way ANOVA (**A**, **C**, **E**). Full data can be found in **Fig. S3 and Fig. S4**.

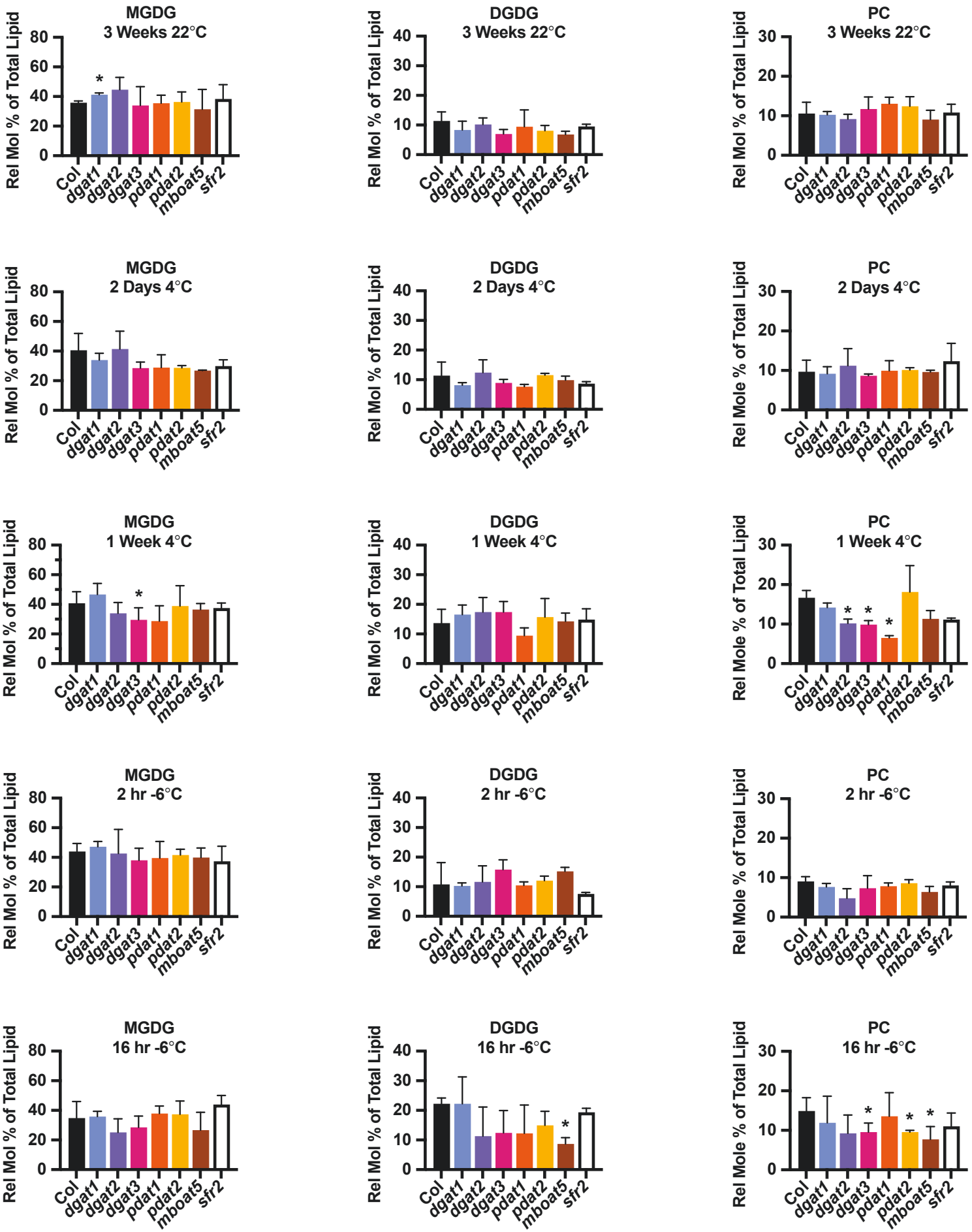

Fig. S1: Relative mole percents of MGDG, DGDG, and PC following the low-temperature step. The data show here was used to generate the line graphs in **Figure 5**, and is separated here to view the entire dataset at once. Error bars represent standard deviations, and asterisks indicate significance of $P \leq 0.05$ calculated with Brown-Forsythe and Welch one-way ANOVA compared to wild type control. n ≥ 4 biological replicates.

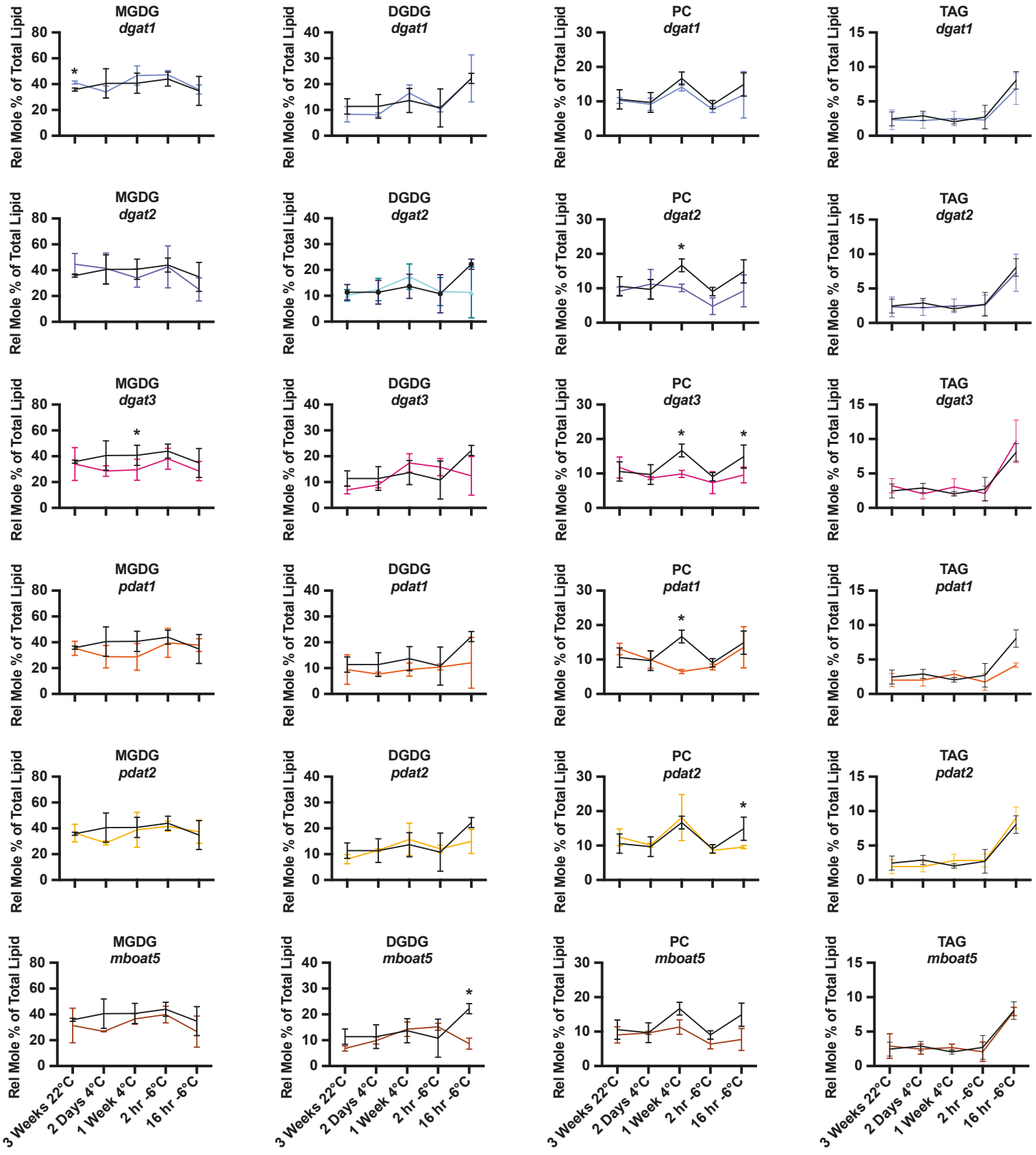

Fig. S2: **Line graphs of the relative mole percents of MGDG, DGDG, PC, and TAG in low-temperature step.** Line graphs show changes in percent of lipid in the acyltransferase mutants compared to the wild type control. One loss of function mutant is shown per graph. Mole percents used were the same as **Fig. S1**, and overlayed graphs can be seen in **Figure 5**. Error bars represent standard deviations, and asterisks indicate significance of $P \leq 0.05$ calculated with Brown-Forsythe and Welch one-way ANOVA compared to wild type control. n ≥ 4 biological replicates.

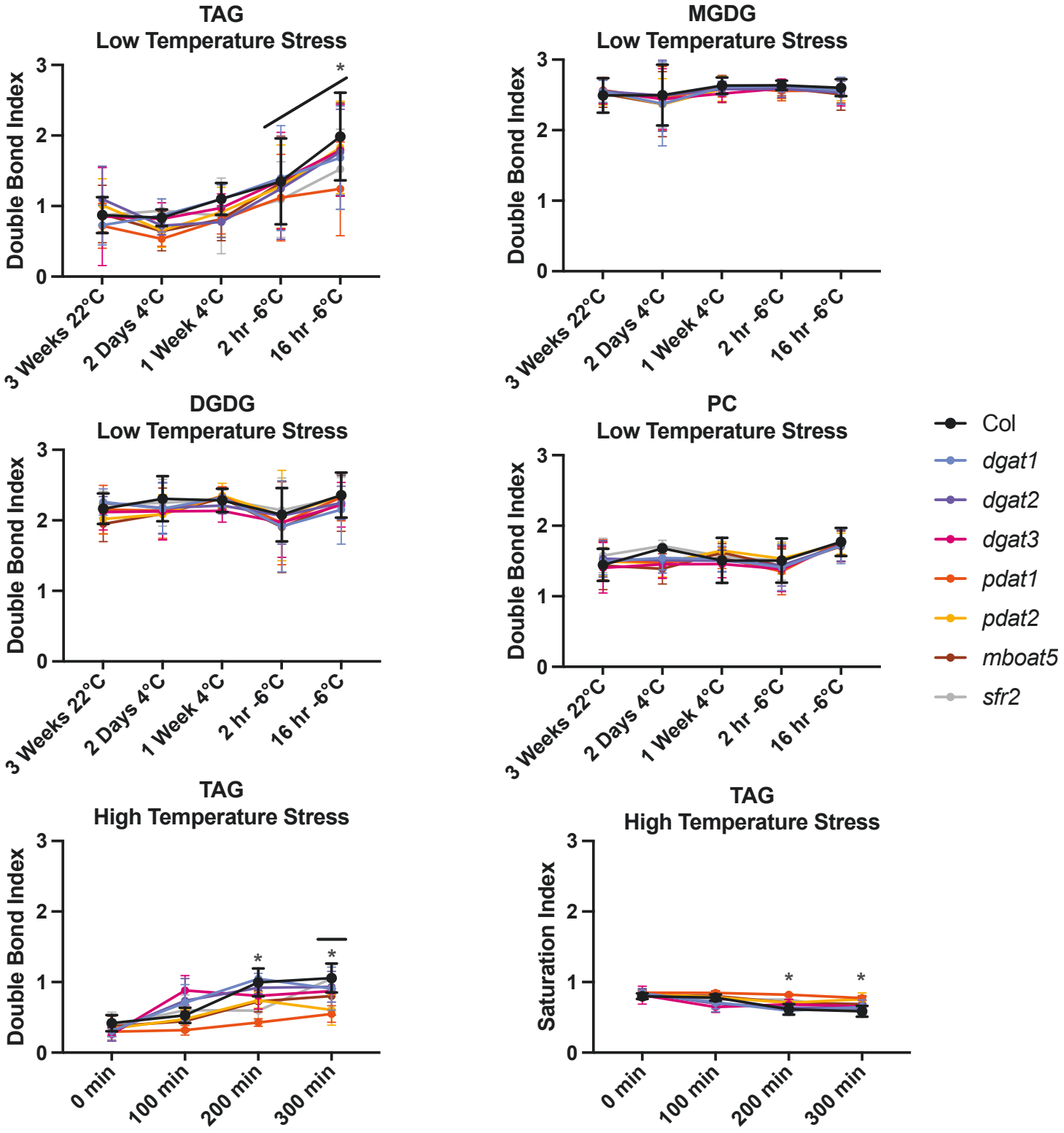

Double Bond Index: ((X:1)*1+(X:2)*2+(X:3)*3)/100, where X represents mol % FA of C16 and C18

Saturation Index: ((16:0) + (18:0))/100, for the mol % FA

Fig. S3: Double bond and saturation index for TAG, MGDG, DGDG, and PC for both the low-temperature step assay, and high-temperature assay. Calculations show were done as described in the *Materials and Methods*. Data includes DBI graphs of *pdat1* TAG, and PC in **Fig. 6** for completeness. Lines above the graphs denote *pdat1* significance at that time point against itself at the start of the assay. Asterisks denote *pdat1* significance to Col at the time point indicated Error bars represent standard deviations, and significance is denoted for $P \leq 0.05$ calculated with Brown-Forsythe and Welch One -Way ANOVA compared to wild type control. n ≥ 2 growth trials with ≥ 2 biological replicates.

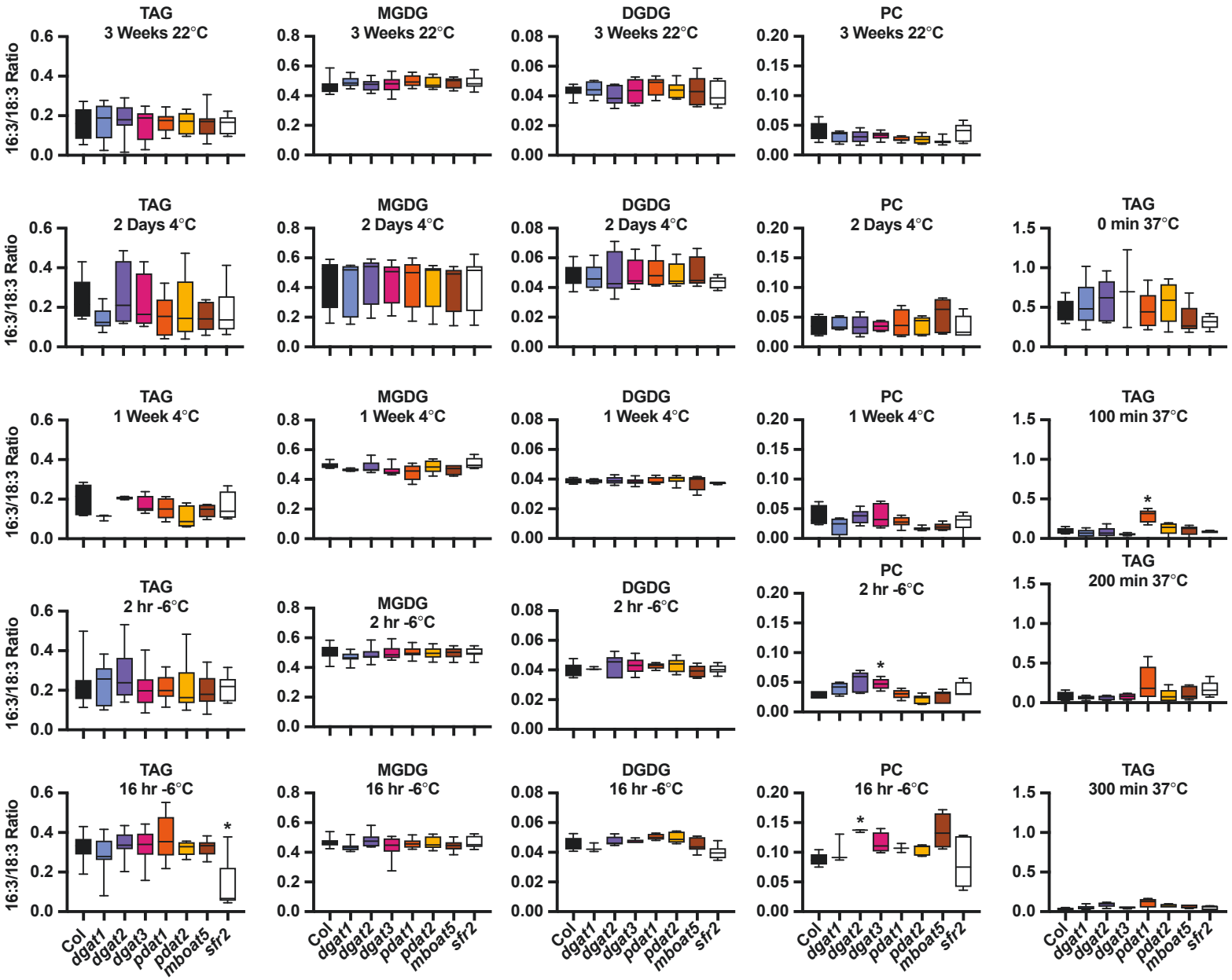

Fig. S4: 16:3/18:3 ratios for TAG, MGDG, DGDG, and PC for the low-temperature assay step and the high-temperature assay. Fatty acid mole percents for 16:3 and 18:3 were used. This figure also includes the graphs in **Fig. 6** for completeness. Error bars represent standard deviations, and asterisks indicate significance of $P \leq 0.05$ calculated with Brown-Forsythe and Welch One-Way ANOVA compared to wild type control.

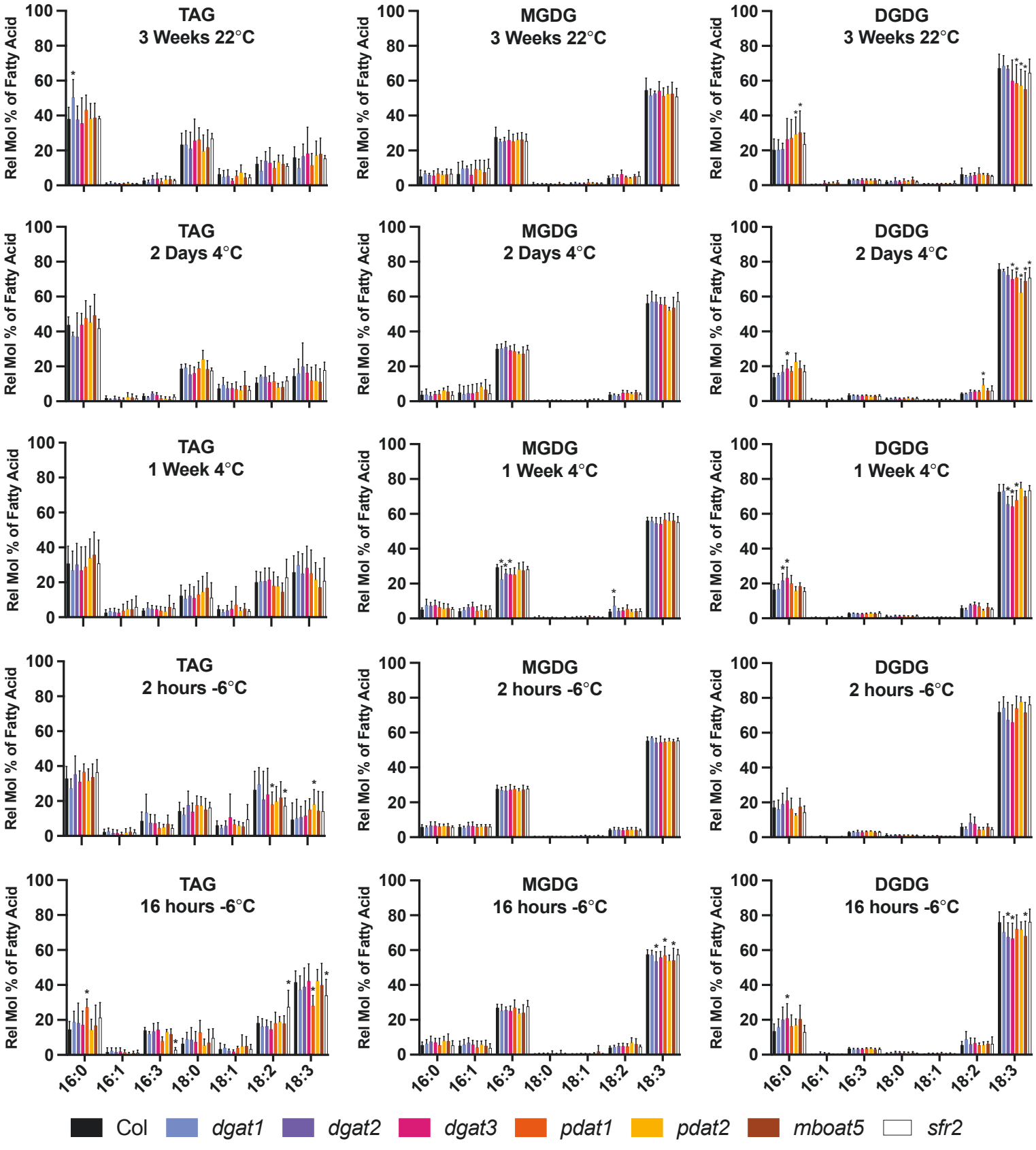

Fig. S5: **Relative mole percent of fatty acids for TAG, MGDG, and DGDG following the low-temperature step assay.** Error bars represent standard deviations, and asterisks indicate significance of $P \leq 0.05$ calculated with Brown-Forsythe and Welch One-Way ANOVA compared to wild type control for each fatty acid species.

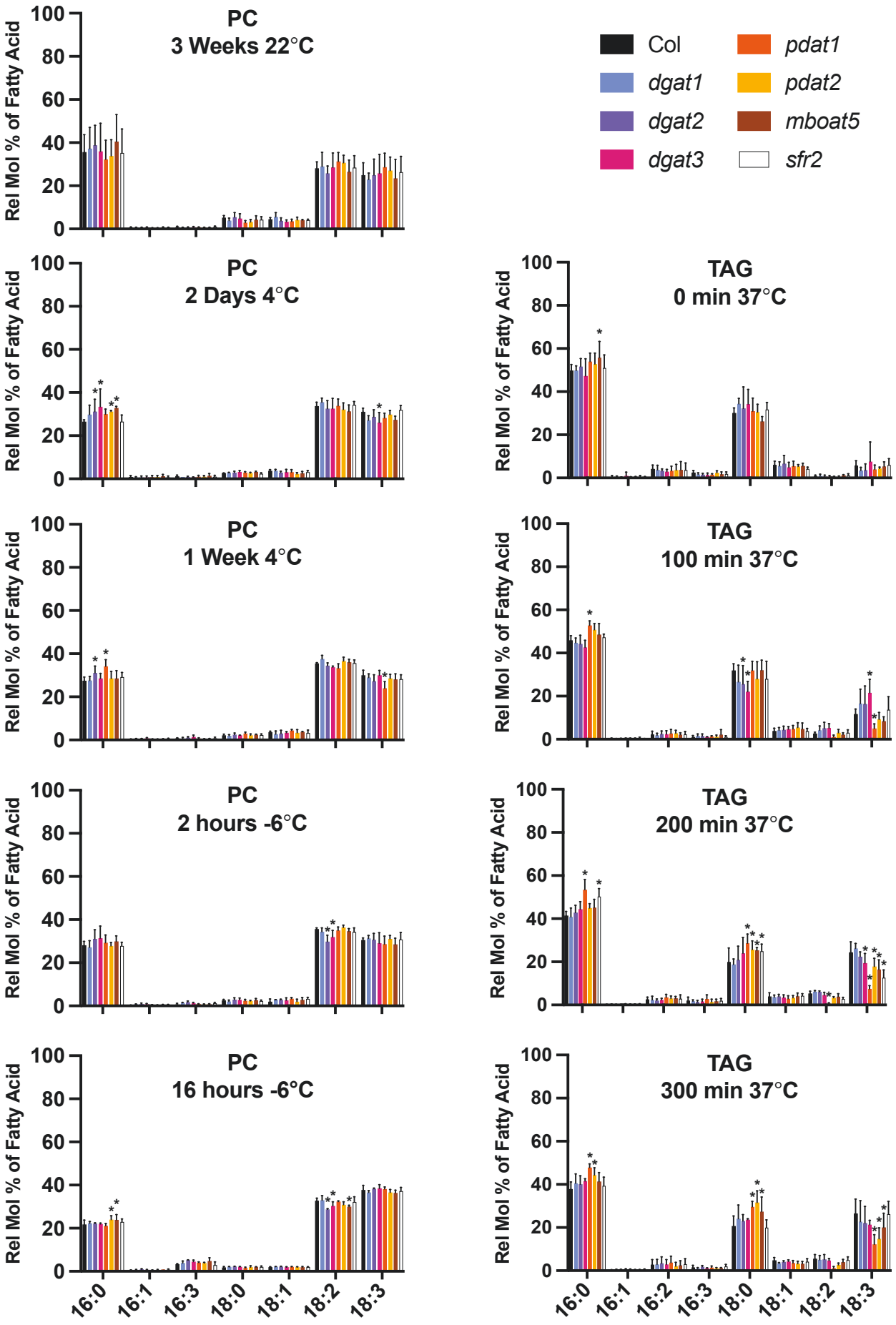

Fig. S6: Relative mole percent of fatty acids for PC in the low-temperature step assay and TAG in the high-temperature assay. Error bars represent standard deviations, and asterisks indicate significance of $P \leq 0.05$ calculated with Brown-Forsythe and Welch One-Way ANOVA compared to wild type control for each fatty acid species.

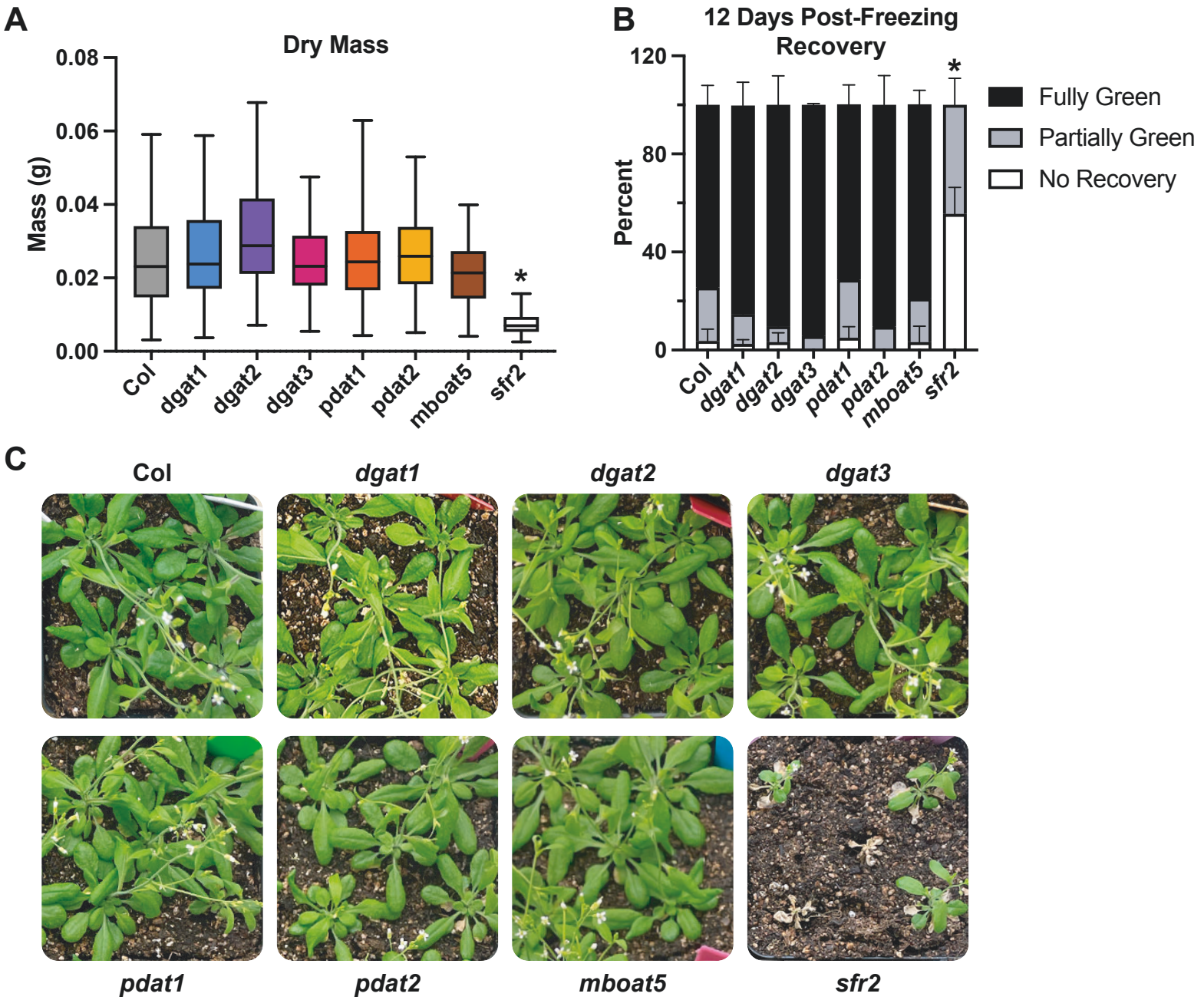

Fig. S7: All acyltransferase mutants are able to recover after a 12-day period. (**A**) Dry weight of individual Arabidopsis plants for all acyltransferase mutants, wildtype and *sfr2* mutants. (**B**) Quantification of the survival of the mutants twelve days after freezing based on manual scoring. (**C**) Photographs of representative pots of recovered mutants taken after twelve days of regrowth. n ≥ 49 individual plants grown across four growth trials. Error bars show standard deviations, and asterisks show significance of $P \leq 0.05$ using two-way ANOVA compared to wild type control.

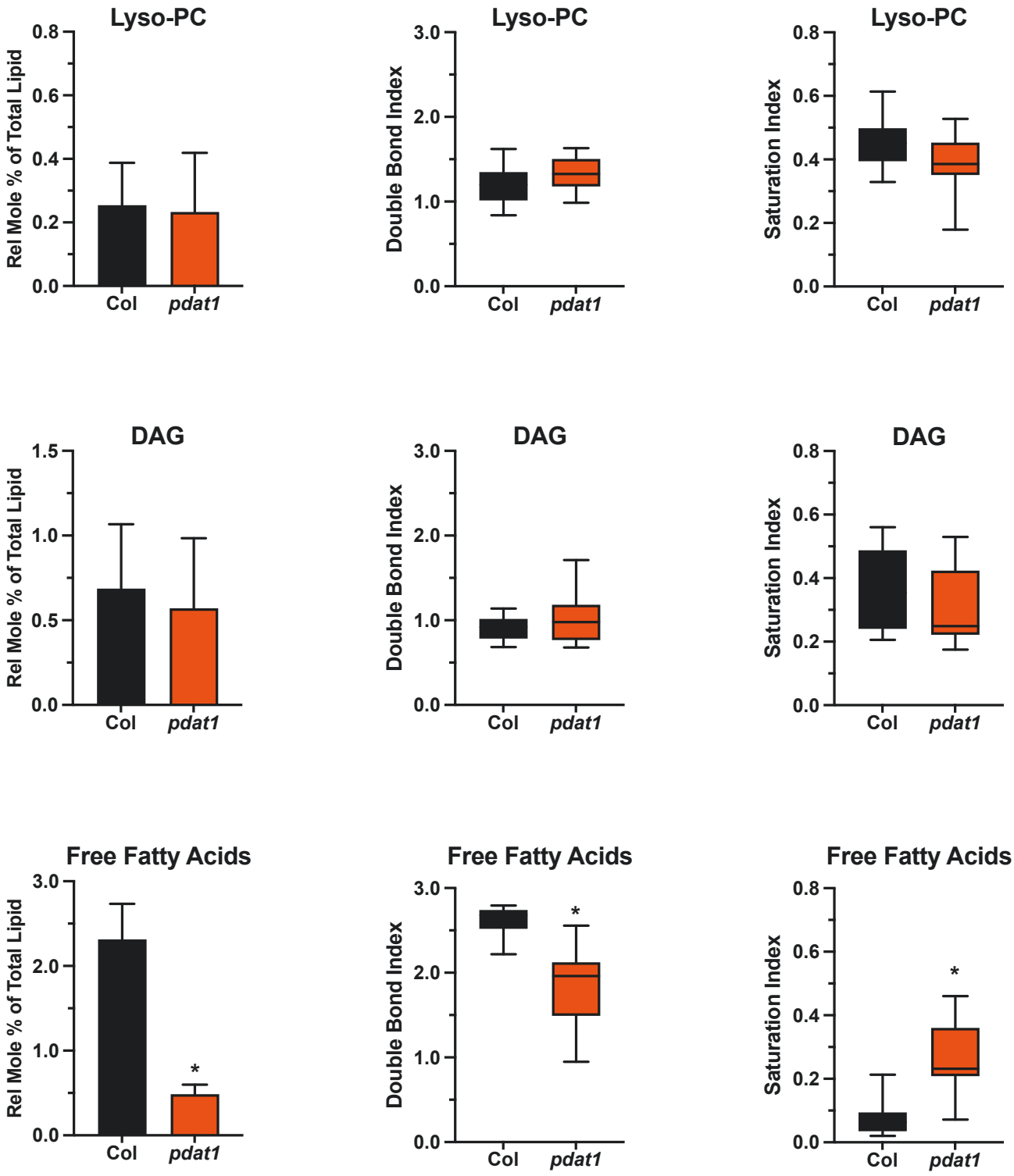

Fig. S8: Relative mole percents, doiuble bond, and saturation indicies for lyso-PC, DAG, and free fatty acids after sixteen hours of freezing. All samples were taken after treatment with 16 hours at -6°C following the low-temperature step depicted in **Figure 1B**. Error bars represent standard deviations, and asterisks indicate significance of $P \leq 0.05$ calculated with an unpaired t test with Welch's correction. n ≥ 11 biological replicates taken over four growth trials.

Table S1: Primers used for genotyping loss-of-function mutants		
	Forward (5'-3')	**Reverse (5'-3')**
DGAT1 Salk	CGACCGTCGGTTCCAGCTCATCGG	GCGGCCAATCTCGCAGCGATCTTG
DGAT2 Salk	GATATGGGTGGTTCCAGAGAGTTC	TCAAAGAATTTTCAGCTCAAGATCATA
DGAT3 Gabbi	CGCTTAAGGCTCAAGTCACAC	TCACAACTCTAACGTTTGGGC
PDAT1 Salk	CATGTGGTGTTGCATTTTCAG	TTTTGTTTTCGGTCTTGTTGG
PDAT2 Salk	CTTTCTCGGCTCATTTCATTG	TTCCATAACACCGAGGTATGC
MBOAT5 (AT2) Salk	CGATCAAGAACCTTTAAGCCC	GCTGAAATCCAAAGCTTGATG
SFR2-3 Salk	GAGCTTGATGTTCTGGAACT	TTGAACTTTGAGCTGTCG
T-DNA Left Boarder Primer for Salk Lines (LBb1.3)	ATTTTGCCGATTTCGGAAC	
GABBI Left Boarder	CCCATTTGGACGTGAATGTAGACAC	

Supplemental Table S2: Average Scoring Percents of Leaf Damage Two Days Post-Freezing								
	Average Percents							
Score	Col	*sfr2*	*dgat1*	*dgat2*	*dgat3*	*pdat1*	*pdat2*	*mboat5*
Level 1 (least severe)	83%	1%	99%	77%	83%	35%	88%	84%
Level 2	16%	17%	1%	21%	17%	43%	12%	15%
Level 3 (most severe)	1%	82%	0%	1%	0%	23%	1%	1%